

MECHANICAL PROPERTIES OF CERAMICS TILES BY REPLACEMENT OF
QUARTZ BY RHA AND POFA

HASSAN USMAN JAMO

A thesis submitted in partial
fulfilment of the requirements for the award of the
Doctor of Philosophy in Science

Faculty of Science, Technology and Human Development
Universiti Tun Hussein Onn Malaysia

JUNE, 2015

ABSTRACT

Rice husk ash (RHA) and palm oil fuel ash (POFA) have a great potential to replace the quartz element in porcelain composition. RHA and POFA were mostly used by construction industries, and only a few researchers studied its applications in ceramics industries. It is due to the mechanical properties of porcelain are strongly affected by the generated thermal stress during processing because of the deleterious effects of quartz. In this work, the quartz is being replaced by RHA, POFA and the combination of RHA and POFA. The sample's composition was mixed for 90 minutes and pressed at different mold pressures (31, 61, 91 and 121 MPa) and then sintered at the sintering temperatures ranging from 1000 to 1300 °C at different soaking times ranging from 1 to 3 hours respectively. The samples were measured the physical and mechanical properties and then the microstructure observation. It was found that the RHA, POFA and the combination of RHA and POFA have tremendous effects on the properties of porcelain tiles. For the RHA, the highest bulk density (2.42 g/cm³) and compressive strength (44 MPa) were recorded on 20 wt% of RHA at the sintering temperature of 1200 °C and the soaking time of 2 hours. For the POFA, the highest bulk density (2.45 g/cm³) and compressive strength (46 MPa) were achieved on 15 wt% of POFA at the sintering temperature of 1100 °C and the soaking time of 2 hours. For the combination of RHA and POFA, the highest bulk density (2.43 g/cm³) and compressive strength (45 MPa) were recorded on 20 wt% of RHA and POFA at the sintering temperature of 1200 °C and the soaking time of 2 hours. It was observed that the microstructure was enhanced by increasing the sintering temperature, mould pressure and soaking time. It can be concluded that samples containing POFA attained vitrification stage at lower temperature and exhibited higher mechanical properties. Thermal expansion and thermal conductivity measurement are some of the areas that could be explored for further research.

ABSTRAK

Abu sekam padi (ASP) dan abu bakar kelapa sawit (ABKS) mempunyai potensi yang besar untuk menggantikan kuartz dalam komposisi porselin. Kebanyakan ASP dan ABKS digunakan oleh industri pembinaan, kecuali hanya beberapa penyelidik sahaja yang mengkaji penggunaannya dalam industri seramik. Ini adalah disebabkan oleh sifat mekanik porselin yang amat dipengaruhi oleh tekanan terma yang terhasil semasa pemrosesan kerana wujud kesan yang merosakkan kuartz. Dalam kajian ini, kuartz digantikan dengan ASP, ABKS dan kombinasi ASP dan ABKS. Komposisi sampel dicampurkan selama 90 minit dan ditekan pada tekanan acuan yang berbeza (31, 61, 91 dan 121 MPa) dan disinter pada suhu di antara 1000 °C hingga 1300 °C pada masa rendaman yang berbeza, masing-masing antara 1 hingga 3 jam. Sampel itu diukur sifat fizikal dan mekanikal dan kemudiannya dibuat pemerhatian mikrostruktur. Hasil kajian menunjukkan bahawa ASP, ABKS dan kombinasi ASP dan ABKS mempunyai kesan yang sangat baik pada sifat-sifat porselin. Untuk ASP, ketumpatan pukal (2.42 g/cm^3) dan kekuatan mampatan (44 MPa) tertinggi dicatatkan pada 20 % berat ASP pada suhu sinter 1200 °C dan pada masa rendaman 2 jam. Untuk ABKS, ketumpatan pukal (2.45 g/cm^3) dan kekuatan mampatan (46 MPa) tertinggi telah dicapai pada 15% berat ABKS pada suhu sinter 1100 °C dan masa rendaman 2 jam. Untuk kombinasi ASP dan POFA, ketumpatan pukal (2.43 g/cm^3) dan kekuatan mampatan (45 MPa) dicatatkan pada 20% berat ASP dan ABKS pada suhu sinter 1200 °C dan pada masa rendaman 2 jam. Ini dapat diperhatikan bahawa peningkatan dalam suhu sinter, tekanan acuan dan merendam masa meningkatkan mikrostruktur. Kesimpulannya, sampel yang mengandungi ABKS mencapai peringkat pengkacaan pada suhu yang lebih rendah dan mempamerkan sifat mekanikal yang lebih tinggi. Pengukuran pengembangan dan kekonduksian terma adalah beberapa bidang yang boleh diterokai untuk penyelidikan selanjutnya.

TABLE OF CONTENT

	SUPERVISOR’S DECLARATION	ii
	TITLE	iii
	STUDENT’S DECLARATION	iv
	DEDICATION	v
	ACKNOWLEDGEMENT	vi
	ABSTRACT	viii
	ABSRAK	ix
	TABLE OF CONTENT	x
	LIST OF FIGURES	xvi
	LIST OF TABLES	xxvii
	LIST OF ABBREVIATIONS	xxix
CHAPTER 1	INTRODUCTION	1
	1.1 Background of the study	1
	1.2 Problem statement	3
	1.3 Objectives of the study	5
	1.4 Scope of the study	5
CHAPTER 2	LITERATURE REVIEW	7
	2.1 Introduction on porcelain ceramic tile	7
	2.1.1 Raw materials of porcelain	7
	2.1.2 Strength consideration	9
	2.1.3 Sintering of porcelain	10
	2.1.4 Sintering stages	12
	2.2 Characterisation	27
	2.2.1 X-ray diffraction	27
	2.2.2 Microstructure observation	32
	2.3 Physical properties	37

2.3.1	Shrinkage	37
2.3.2	Percentage of porosity	42
2.3.3	Bulk density	45
2.4	Mechanical properties	50
2.4.1	Bending strength	50
2.4.2	Vickers hardness	55
2.4.3	Compressive strength	57
2.5	Rice husk ash (RHA)	59
2.5.1	High silica content with amorphous characteristics	59
2.5.2	Disposal problems	60
2.6	Origin of palm oil	61
2.6.1	Palm oil fuel ash (POFA)	62
2.6.2	Environmental issues	64
2.6.3	Summary	65
CHAPTER 3	RESEARCH METHODOLOGY	66
3.1	Introduction	66
3.2	Research Design	68
3.2.1	Effects of substitution of quartz by RHA	68
3.2.2	Effects of substitution of quartz by POFA	68
3.2.3	Effects of substitution of quartz by the combination of RHA and POFA	69
3.3	Experimental design variables	69
3.3.1	Experimental parameters	69
3.4	Preparation of raw materials	78
3.4.1	RHA	78
3.4.2	POFA	79
3.5	Sample preparation	79
3.5.1	Sample composition	79
3.5.2	Mixing	80
3.5.3	Dry pressing	80
3.5.4	Drying	81
3.5.5	Sintering	81

3.6	Physical measurement	81
3.6.1	Volume shrinkage	81
3.6.2	Porosity and bulk density	82
3.7	X-ray Fluorescence characterisation measurement	83
3.7.1	X-ray diffraction (XRD) measurement	83
3.8	Scanning electron microscopy (SEM)	84
3.9	Mechanical measurement	84
3.9.1	Vickers hardness	84
3.9.2	Bending strength	85
3.9.3	Compressive strength	86
3.10	Particle size analysis	87
	The powder was diluted using water, the solution was placed into the machine, the machine stirred the solution for 5 to 7 minutes in a chamber having two lasers. With the help of a formula built in the machine the sizes of the particles were analysed	87
3.11	Etching	87
CHAPTER 4	RESULTS AND DISCUSSIONS	88
4.1	Introduction	88
4.2	Analysis of raw materials	88
4.2.1	X-ray fluorescence (XRF) measurement	88
4.2.2	X-ray diffraction (XRD) analysis	89
4.2.3	Particle size analysis	91
	4.2.3.1 Porcelain raw material	91
	4.2.3.2 RHA	91
	4.2.3.3 POFA	91
4.2.4	Scanning electron microscopy (SEM)	95
4.3	Phase I: Study of RHA	96
4.3.1	Effects of sintering temperature, mould pressure and soaking on volume shrinkage	96
4.3.2	Effects of sintering temperature, mould pressure and soaking time on percentage porosity	100

4.3.3	Effects of sintering temperature, mould pressure and soaking time on bulk density	103
4.3.4	Effects of RHA, sintering temperature, mould pressure and soaking time on Vickers hardness	106
4.3.5	Effects of sintering temperature, mould pressure and soaking time on bending strength	109
4.3.6	Effects of sintering temperature, mould pressure and soaking time on compressive strength	112
4.3.7	Effects of sintering temperature, mould pressure and soaking time on XRD	116
4.3.8	Effects of sintering temperature, mould pressure and soaking time on microstructure	119
4.3.9	Summary	122
4.4	Phase II Study of POFA, sintering temperature, mould pressure and soaking	123
4.4.1	Effects of sintering temperature, mould pressure and soaking time on volume shrinkage	123
4.4.2	Effects of sintering temperature, mould pressure and soaking time on percentage of porosity	125
4.4.3	Effects of sintering temperature and soaking time on bulk density	128
4.4.4	Effects of sintering temperature and soaking time on Vickers hardness	132
4.4.5	Effects of sintering temperature and soaking time on bending strength	135
4.4.6	Effects of sintering temperature and soaking time on compressive strength	139
4.4.7	Effects of sintering temperature and soaking time on XRD	142
4.4.8	Effects of sintering temperature and soaking time on microstructure	145

4.4.9	Summary	148
4.5	Phase III: Study of RHA and POFA	150
4.5.1	Effects of sintering temperature and soaking time on volume shrinkage	150
4.5.2	Effects of sintering temperature and soaking time on percentage of porosity	152
4.5.3	Effects of sintering temperature and soaking time on bulk density	155
4.5.4	Effects of sintering temperature and soaking time on Vickers hardness	158
4.5.5	Effects of sintering temperature and soaking time on bending strength	161
4.5.6	Effects of sintering temperature and soaking time on compressive strength	164
4.5.7	Effects of sintering temperature and soaking time on XRD	167
4.5.8	Effects of sintering temperature and soaking time on microstructure	171
4.5.9	Summary	173
4.5.10	Relationship between percentage of porosity and compressive strength	174
4.5.11	Discussion on comparison between samples containing RHA, POFA and the combination of RHA and POFA	177
CHAPTER 5	CONCLUSION AND RECOMMENDATIONS	181
5.1	Conclusion	181
5.2	Recommendation	183
REFERENCES		184

LIST OF FIGURES

Figure 2.1:	Stages of sintering (a) free particles, (b) necking between particles, (c) formation of grain boundary, and (d) densification process and pores elimination (Randal, 1991)	13
Figure 2.2:	XRD curves of fired body mixes (Prasad <i>et al.</i> , 2001)	28
Figure 2.3:	XRD results of porcelains, sintered at 1350 °C and 1400 °C. (Karamanov <i>et al.</i> , 2006)	29
Figure 2.4:	X-ray diffraction patterns of POFA20 tile and sintered at different temperatures (Tonnayopas <i>et al.</i> , 2009)	30
Figure 2.5:	X-ray diffraction patterns: (a) 20G, 1150 °C; (b) 15G, 1200 °C; (c) 20F10G, 1200 °C; and (d) 25 F5G, 1220 °C (Luz and Ribeiro, 2007)	31
Figure 2.6:	X-ray diffractogram of the fired porcelain body at different mould pressure (MP) (Pérez <i>et al.</i> , 2012)	32
Figure 2.7:	SEM images of the pellets after (a) 1000°C, (b) 1100°C, (c) 1200°C, (d)1300°C, (e) 1400°C	33
Figure 2.8:	Backscattered image of the fractured surfaces of POFA-GFQW tiles (Tonnayopas <i>et al.</i> , 2009)	34
Figure 2.9:	SEM of light weight porcelain stoneware Garcia-Ten <i>et al.</i> , (2012)	35
Figure 2.10:	SEM observations on polished surfaces of the porcelain stoneware (Martín-Márquez <i>et al.</i> , 2010a)	36
Figure 2.11:	SEM micrographs on polished surfaces of the porcelain stoneware at different mould pressures: 10 MPa (b) 20 MPa, (c) 30 MPa and (d) 30 MPa (Preze <i>et al.</i> , 2012)	37

Figure 2.12:	Effect of RHA+SF on the fired shrinkage of body mixes fired at different test temperature (Prasad <i>et al.</i> , 2003)	38
Figure 2.13:	Linear shrinkage % of the understudied compositions as function of maximum firing temperature (Leonelli <i>et al.</i> , 2001)	39
Figure 2.14:	Linear shrinkage as function of temperature (Martín-Márquez <i>et al.</i> , 2008)	40
Figure 2.15:	Linear shrinkage as a function of the firing temperatures for the tested samples (Tucci <i>et al.</i> , 2007)	40
Figure 2.16:	Firing shrinkage as function of firing temperature (de’Gennaro <i>et al.</i> , 2003)	41
Figure 2.17:	Dilatometric sintering curves of C0 (standard sample) and C1 (sample with cathode ray TV) compositions (de’Gennaro <i>et al.</i> , 2003)	42
Figure 2.18:	Influence of firing temperature on porosity and irreversible stain retention (evaluated as E) for samples obtained from the as-received industrial powder (Sanchez <i>et al.</i> 2001).	43
Figure 2.19:	Total porosity (PT), closed porosity (PC), and open porosity (PO) porosities behaviour vs. temperature for laboratory fired standard sample (C0). (Andreola <i>et al.</i> 2008)	43
Figure 2.20:	The variations of total porosity as function of soaking time for STD milled at 8 h and sintered at three different temperatures. (Salem <i>et al.</i> , 2010)	44
Figure 2.21:	Apparent porosity as a function of temperature (Dana <i>et al.</i> , 2004).	45
Figure 2.22:	Bulk densities of porcelain compositions (Kamseu <i>et al.</i> , 2007)	46
Figure 2.23:	Bulk density versus oil palm fuel ash POFA content (Tonayopas <i>et al.</i> , 2009)	46
Figure 2.24:	Absolute and bulk densities of green tiles at different MP (Pérez <i>et al.</i> , 2011)	47
Figure 2.25:	Variation in bulk density of C1 and C2 bodies with heating temperature (Das and Dana, 2003)	48
Figure 2.26:	Bulk density versus the sintering temperature. NC: Samples without calcinations, C: calcined samples (Kitouni and Harabi, 2011)	48

Figure 2.27: Effect of MP and firing temperature on the maximum density (Youssef and Ghazal, 2011)	49
Figure 2.28: Bending strength of porcelain compositions (Kamseu <i>et al.</i> , 2007)	50
Figure 2.29: Effect of RHA on the fired M.O.R. of body mixes fired at different test temperatures. (Prasad <i>et al.</i> , 2001)	51
Figure 2.30: Bending strength of porcelain compositions (Kamseu <i>et al.</i> , 2007)	52
Figure 2.31: Bending strength versus oil palm fuel ash (OPFA) content (Tonnyapas <i>et al.</i> , 2009)	53
Figure 2.32: Flexural strength and tensile and versus sintering temperature for calcined porcelain samples (Kitouni and Harabi, 2011)	54
Figure 2.33: Effect of temperature and soaking time on the MOR of samples (Youssef and Ghazal, 2011)	54
Figure 2.34: Vickers hardness versus POFA content (Tonnyapas <i>et al.</i> , 2009)	55
Figure 2.35: Effect of MP and soaking time on Rockwell Hardness for samples fired at 1250 °C (Youssef and Ghazal, 2011)	56
Figure 2.36: Variation of Vickers hardness with Weight % RHA (Prasad and Krishna, 2011)	56
Figure 2.37: Vickers hardness versus RHA content (Fadzil <i>et al.</i> , 2008)	57
Figure 2.38: Effect of firing temperature and soaking time on the cold crushing strength of samples (Youssef and Ghazal, 2011)	58
Figure 2.39: Dry compressive strength of fired briquettes as a function of OBM content as well as firing temperatures (El-mahllawy and Osman, 2010)	58
Figure 2.40: Map of the largest palm oil producing countries in the world (Zuur, 2004)	61
Figure 33.1: Overall flow Chart for the experiment	67
Figure 4.1: The XRD patterns of raw materials (where c = cristobalite, cc = calcite, k = kaolin, m = mullite, mu = muscovite, p = portlandite, q = quartz)	90
Figure 4.2: Result of particle size analysis of porcelain raw material	92
Figure 4.3: Result of particle size analysis of RHA	93

Figure 4.4:	Result of particle size analysis of POFA	94
Figure 4.5:	Surface morphology of (a) RHA (b) POFA (c) ceramic (porcelain) raw material. Phase 1: Substitution of quartz by RHA	95
Figure 4.6:	Effect of temperature on shrinkage of the samples with different percentage of RHA (mould pressure =91 MPa, soaking time =2 hours)	99
Figure 4.7:	Effect of mould pressure on shrinkage of the samples with different percentage of RHA (temperature =1200 °C, soaking time =2 hours)	99
Figure 4.8:	Effect of soaking time shrinkage of the samples with different percentage of RHA (temperature =1200 °C, mould pressure = 91 MPa)	99
Figure 4.9:	Effect of temperature on percentage of porosity of the samples with different percentage of RHA (mould pressure =91 MPa, soaking time =2 hours)	101
Figure 4.10:	Effect of mould pressure on percentage of porosity the samples of sample with different percentage of RHA (temperature =1200 °C, soaking time =2 hours)	101
Figure 4.11:	Effect of soaking time on percentage of porosity of the samples with different percentage of RHA (temperature =1200 °C, mould pressure = 91 MPa)	101
Figure 4.12:	Effect of temperature on bulk density of the samples with different percentage of RHA (mould pressure =91 MPa, soaking time =2 hours)	104
Figure 4.13:	Effect of mould pressure on bulk density of the samples with different percentage of RHA (temperature =1200 °C, soaking time =2 hours)	104
Figure 4.14:	Effect of soaking time on bulk density of body mixes with different percentage of RHA (temperature =1200 °C, mould pressure = 91 MPa)	104
Figure 4.15:	Effect of temperature on Vickers micro-hardness of sample with different percentage of RHA (mould pressure =91 MPa, soaking time =2 hours)	108

- Figure 4.16: Effect of mould pressure on hardness of the samples with different percentage of RHA (temperature =1200 °C, soaking time =2 hours) 108
- Figure 4.17: Effect of soaking time on Vickers hardness of the samples with percentage of RHA (temperature =1200 °C, mould pressure = 91 MPa) 108
- Figure 4.18: Effect of temperature on bending strength of the samples with different percentage of RHA (mould pressure =91 MPa, soaking time =2 hours) 111
- Figure 4.19: Effect of mould pressure on bending strength of the samples with different percentage of RHA (temperature =1200 °C, soaking time =2 hours) 111
- Figure 4.20: Effect of soaking time on bending strength of the samples with different percentage of RHA (temperature =1200 °C, mould pressure = 91 MPa) 111
- Figure 4.21: Effect of temperature on compressive strength of the samples with different percentage of RHA (mould pressure =91 MPa, soaking time =2 hours) 114
- Figure 4.22: Effect of mould pressure on compressive strength of the samples with different percentage RHA (temperature =1200 °C, soaking time =2 hours) 114
- Figure 4.23: Effect of soaking time compressive strength of the samples with different percentage of RHA (temperature =1200 °C, mould pressure = 91 MPa) 114
- Figure 4.24: The XRD curves of the samples containing 20 wt% of RHA sintered at different temperatures (mould pressure =91 MPa, soaking time =2 hours) 116
- Figure 4.25: The XRD curves of sintered sample containing 20 wt% RHA pressed at different mould pressure (temperature =1200 °C, soaking time =2 hours) 117
- Figure 4.26: The XRD curves of the samples containing 20 wt% RHA sintered at different soaking times (temperature =1200 °C, mould pressure = 91 MPa) 118

- Figure 4.27: The SEM of the samples containing 20 wt% of RHA sintered at different temperatures of (a) 1000 °C (b) 1100 °C (c) 1200 °C (d) 1300 °C. All micrograph were taken with 1000X magnification (mould pressure =91 MPa, soaking time =2 hours) 119
- Figure 4.28: SEM of the samples sintered containing 20 wt% RHA pressed at mould pressure of (a) 31 MPa (b) 61 MPa (c) 91 MPa (d) 121MPa: All micrographs were taken with 1000X magnification 120
- Figure 4.29: SEM of the samples sintered containing 20 wt% RHA sintered at a soaking time of (a) 1 Hour (b) 2 Hours (c) 3 Hours. All micrograph were taken with 1000X magnification (temperature =1200 °C, mould pressure = 91 MPa) 121
- Figure 4.30: Effect of temperature on shrinkage of the samples with different percentage of POFA (mould pressure =91 MPa, soaking time =2 hours) 124
- Figure 4.31: Effect of mould pressure on shrinkage of the samples with different percentage of POFA (temperature =1100 °C, soaking time =2 hours) 124
- Figure 4.32: Effect of soaking time of shrinkage of body mixes with different percentage of POFA (temperature =1100 °C, mould pressure = 91 MPa) 124
- Figure 4.33: Effect of temperature on percentage of porosity of the samples with different percentage of POFA wt% (mould pressure =91 MPa, soaking time =2 hours) 127
- Figure 4.34: Effect of mould pressure on percentage of the samples of sample with different percentage of POFA (temperature =1100 °C, soaking time =2 hours) 127
- Figure 4.35: Effect of soaking time of percentage of porosity of the samples with different percentage of POFA (temperature =1100 °C, mould pressure = 91 MPa) 127
- Figure 4.36: Effect of temperature on bulk density of the samples with different percentage of POFA (mould pressure =91 MPa, soaking time =2 hours) 130

- Figure 4.37: Effect of mould pressure on bulk density of the samples with different percentage of POFA (temperature =1100 °C, soaking time =2 hours) 130
- Figure 4.38: Effect of soaking time on bulk density of the samples with different percentage of POFA (temperature =1100 °C, mould pressure = 91 MPa) 130
- Figure 4.39: Effect of temperature on Vickers hardness of the samples with different percentage of POFA (mould pressure =91 MPa, soaking time =2 hours) 134
- Figure 4.40: Effect of mould pressure on Vickers hardness of the samples with different percentage of RHA (temperature =1100 °C, soaking time =2 hours) 134
- Figure 4.41: Effect of soaking time on Vickers hardness of the the samples with different percentage of POFA (temperature =1100 °C, mould pressure = 91 MPa) 134
- Figure 4.42: Effect of temperature on bending strength of body the samples different percentage of POFA (mould pressure =91 MPa, soaking time =2 hours) 137
- Figure 4.43: Effect of mould pressure on bending strength of the samples with different percentage of POFA (temperature =1100 °C, soaking time =2 hours) 137
- Figure 4.44: Effect of soaking time on bending strength of the the samples with different percentage of POFA (temperature =1100 °C, mould pressure = 91 MPa) 137
- Figure 4.45: Effect of temperature on compressive strength of the samples with different percentage of POFA (mould pressure =91 MPa, soaking time =2 hours) 140
- Figure 4.46: Effect of mould pressure on compressive strength of the samples with 140
- Figure 4.47: Effect of soaking time on compressive strength of the samples with different percentage of POFA (temperature =1100 °C, mould pressure = 91 MPa) 140

- Figure 4.48: The XRD curves of the samples containing 15 wt% of POFA sintered at different temperatures (mould pressure =91 MPa, soaking time =2 hours) 143
- Figure 4.49: The XRD curves of the samples containing 15 wt% POFA pressed at different mould pressure (temperature =1100 °C, soaking time =2 hours) 144
- Figure 4.50: The XRD curves of the samples containing 15 wt% POFA sintered at different soaking times ((temperature =1100 °C, mould pressure = 91 MPa) 145
- Figure 4.51: SEM of the sample containing 15 wt% POFA sintered at a temperature of (a) 1000 °C (b) 1100 °C (c) 1200 °C (c) 1280 °C. All micrograph were taken with 1000X magnification (mould pressure =91 MPa, soaking time =2 hours) 146
- Figure 4.52: SEM of the samples sintered containing 15 wt% POFA pressed at pressed at mould pressure of (a) 31 MPa (b) 61 MPa (c) 91 MPa (d) 121 MPa. All micrograph were taken with 1000X magnification (temperature =1100 °C, soaking time =2 hours) 147
- Figure 4.53: SEM of the samples containing 15 wt% of POFA sintered at a soaking time of (a) 1hour (b) 2hours (c) 3hours. 1000X magnification (temperature =1100 °C, mould pressure = 91 MPa) 148
- Figure 4.54: Effect of temperature on shrinkage of the samples with different percentage of RHA and POFA (mould pressure =91 MPa, soaking time =2 hours) 151
- Figure 4.55: Effect of mould pressure on shrinkage of the samples with different percentage of RHA and POFA (temperature =1200 °C, soaking time =2 hours) 151
- Figure 4.56: Effect of soaking time on shrinkage of the samples with different percentage of RHA and POFA (temperature =1200 °C, mould pressure =91 MPa) 151
- Figure 4.57: Effect of temperature on percentage of porosity of the samples with different percentage of RHA and POFA (mould pressure =91 MPa, soaking time =2 hours) 154

- Figure 4.58: Effect of mould pressure on percentage of the samples of sample with different percentage of RHA and POFA wt% (temperature =1200 °C, soaking time =2 hours) 154
- Figure 4.59: Effect of soaking time on the porosity of of the samples with different percentage of RHA and POFA (temperature =1200 °C, mould pressure =91 MPa) 154
- Figure 4.60: Effect of temperature on bulk density of the samples with different percentage of RHA and POFA (mould pressure =91 MPa, soaking time =2 hours) 157
- Figure 4.61: Effect of mould pressure on bulk density of the samples with different percentage of RHA and POFA (temperature =1200 °C, soaking time =2 hours) 157
- Figure 4.62: Effect of soaking time on the bulk density of the samples with different percentage of RHA and POFA (temperature =1200 °C, mould pressure =91 MPa) 157
- Figure 4.63: Effect of temperature on Vickers micro-hardness of sample with different percentage of RHA (mould pressure =91 MPa, soaking time =2 hours) 159
- Figure 4.64: Effect of mould pressure on Vickers hardness of the samples with different percentage of RHA and POFA (temperature =1200 °C, soaking time =2 hours) 159
- Figure 4.65: Effect of soaking time on Vickers hardness of the samples with different percentage of RHA and POFA (temperature =1200 °C, mould pressure = 91 MPa) 159
- Figure 4.66: Effect of temperature on bending strength of the samples with different percentage of RHA and POFA (mould pressure =91 MPa, soaking time =2 hours) 163
- Figure 4.67: Effect of mould pressure bending strength of the samples with different percentage of RHA and POFA (temperature =1200 °C, soaking time =2 hours) 163
- Figure 4.68: Effect of soaking time on bending strength of the samples with different percentage of RHA and POFA (temperature =1200 °C, mould pressure = 91 MPa) 163

- Figure 4.69: Effect of temperature on compressive strength of the samples with different percentage of RHA and POFA (mould pressure =91 MPa, soaking time =2 hours) 165
- Figure 4.70: Effect of mould pressure on compressive strength of the samples with different percentage of RHA and POFA (temperature =1200 °C, soaking time =2 hours) 165
- Figure 4.71: Effect of soaking time on compressive strength of the samples with different percentage of RHA and POFA (temperature =1200 °C, mould pressure = 91 MPa) 165
- Figure 4.72: The XRD curves of the samples containing 20wt% of RHA and POFA sintered at different temperatures (mould pressure =91 MPa, soaking time =2 hours) 168
- Figure 4.73: The XRD curves of the samples containing 20 wt% of RHA and POFA sintered at different mould pressure (temperature =1200 °C, soaking time =2 hours) 169
- Figure 4.74: The XRD curves of the samples containing 20 wt% of RHA and POFA sintered at different soaking time (temperature =1200 °C, mould pressure =91 MPa) 170
- Figure 4.75: SEM of the samples containing 20 wt% RHA and POFA sintered at a temperature of (a) 1000°C (b) 1200°C (c) 1300°C. All micrograph were taken with 1000X magnification (mould pressure =91 MPa, soaking time =2 hours) 171
- Figure 4.76: SEM of the samples containing 20 wt% RHA and POFA pressed at a mould pressure of (a) 31 MPa (b) 61 MPa (c) 91 MPa (d) 121 MPa. All micrograph were taken with 1000X magnification (temperature =1200 °C, soaking time =2 hours) 172
- Figure 4.77: SEM of the samples containing RHA and POFA sintered at a soaking times (a) 1 hour (b) 2 hours (c) 3 hours. All micrograph were taken with 1000X magnification (temperature =1200 °C, mould pressure =91 MPa) 173
- Figure 4.78: Relationship between the compressive strength and percentage of porosity (RHA wt %) 175
- Figure 4.79: Relationship between the compressive strength and percentage of porosity (POFA wt %) 176

Figure 4.80: Relationship between the compressive strength and percentage of porosity (RHA and POFA wt %)

LIST OF TABLES

Table 3.1: RHA wt% Vs temperature	70
Table 3.2: RHA wt% Vs mould pressure	71
Table 3.3: RHA wt% Vs soaking time	72
Table 3.4: POFA wt% Vs temperature	73
Table 3.5: POFA wt% Vs mould pressure	74
Table 3.6: POFA wt% Vs soaking time	75
Table 3.7: RHA and POFA wt% Vs temperature	76
Table 3.8: RHA and POFA wt% Vs mould pressure	77
Table 3.9: RHA and POFA wt% Vs soaking time	78
Table 3.10: The composition with the substitution of quartz by RHA (wt %)	79
Table 3.11: The composition with the substitution of quartz by POFA (wt %)	80
Table 3.12: The composition with the substitution of quartz by RHA and POFA (wt %)	80
Table 4.1: X-Ray Fluorescence (XRF) Analysis	89
Table 4.2: XRD quantitative analysis of the samples containing 20 wt% RHA sintered at different temperatures (mould pressure =91 MPa, soaking time =2 hours)	116
Table 4.3: XRD quantitative analysis of the samples containing 20 wt% RHA pressed at different mould pressure (temperature =1200 °C, soaking time =2 hours)	117
Table 4.4: XRD quantitative analysis of the samples containing 20wt% RHA sintered at different soaking times (temperature =1200 °C, mould pressure = 91 MPa)	118

Table 4.5:	XRD quantitative analysis of the samples containing 15 wt% of POFA sintered at different temperatures (mould pressure =91 MPa, soaking time =2 hours)	143
Table 4.6:	XRD quantitative analysis of the samples containing 15 wt% POFA pressed at different mould pressure (temperature =1100 °C, soaking time =2 hours)	144
Table 4.7:	XRD quantitative analysis of the samples containing 15 wt% POFA sintered at different soaking times (temperature =1100 °C, mould pressure = 91 MPa)	145
Table 4.8:	XRD quantitative analysis of the samples containing 20 wt% of RHA and POFA sintered at different temperatures (mould pressure =91 MPa, soaking time =2 hours)	168
Table 4.9:	XRD quantitative analysis of the samples containing 20 wt% of RHA and POFA pressed at different mould pressure (temperature =1200 °C, soaking time =2 hours)	169
Table 4.10:	XRD quantitative analysis of the samples containing 20 wt% RHA and POFA sintered at different soaking times (temperature =1200 °C, mould pressure =91 MPa)	170

LIST OF ABBREVIATIONS

Al_2O_3	=	Aluminium Oxide
C_2S	=	Dicalcium Silicate
C_3A	=	Tricalcium Aluminate
C_3S	=	Tricalcium Silicate
CaCO_3	=	Calcium Carbonate
CaO	=	Calcium Oxide
Ca(OH)_2	=	Calcium Hydroxide
CaO	=	Calcium Oxide
Fe_2O_3	=	Iron Oxides
SiO_2	=	Silica
MgO	=	Magnesium Oxide
MP	=	Mould Pressure
MPa	=	Mega Pascal
OPC	=	Ordinary Portland Cement
POFA	=	Palm Oil Fuel Ash
RH	=	Rice Husk
RHA	=	Rice Husk Ash
XRD	=	X-ray Diffraction
XRF	=	X-ray fluorescence
A	=	Alpha
B	=	Beta
C-S-H	=	Calcium Silicate Hydrate
Θ	=	Bragg's Angle
Π	=	Pi

CHAPTER 1

INTRODUCTION

1.1 Background of the study

Ceramic tile is a product that stands out for its low water absorption and high mechanical strength. The properties of the product result from its low porosity due to the processing conditions (high degree milling of raw materials, high force compaction and sintering temperature), and the potential of the raw materials to form liquid phases during sintering (high desiccation). However, in the case of polished ceramic, the sealed pores remaining after the manufacturing process may impair some of its technical properties, such as its stain resistance. Porcelain tile is a type of the ceramic materials which have the vitreous characteristics. Vitrification indicates a high degree of melting on firing which confer low (often < 0.5%) porosity and high (> 40%) glass content on fired porcelain (Perez *et al.*, 2013). As the of ceramic material, the porcelains have high hardness, low electrical and thermal conductivities, and brittle fracture (Callister, 2008). Porcelains consists of approximately 50% kaolin [$\text{Al}_2\text{Si}_2\text{O}_5(\text{OH})_4$], 25% silica (SiO_2), and 25% feldspar [$(\text{K},\text{Na})_2\text{O} \cdot \text{Al}_2\text{O}_3 \cdot 6\text{H}_2\text{O}$]. The kaolin provides the plasticity during firing, the feldspar assists in the liquid formation and reduces the porosity, the quartz serves as a binder. This composition makes a material body plasticity and a wide firing temperature range at a relatively low cost (Buchanan 1991 and Olupot, 2006). Porcelain is a type of ceramic highly valued for its beauty and strength. Whiteness, a delicate appearance, and translucence characterize it. It is known primarily material as for high-quality vases, table ware, figures and decorative objects.

Porcelain tiles were introduced at the end of 1980s by Fiandre, one of the leading Italian porcelain tile manufacturers. Among the various types of ceramic

floor and wall tile, porcelain tile is the product which in recent years has shown the greatest rate of increase (on a percent basis) in the amount produced, amount sold, and obviously amount used (Abadir *et al.*, 2002). The American National standard Specifications for Ceramic Tile defines porcelain tiles as: dense, smooth, impervious (with water absorption of 0.5 percent or less), and stain resistant (Ece and Nakagawa, 2002). Their peculiar characteristics put them at the top of a class of available commercial products that can be used for both indoor and outdoor building applications. Since they achieve a very high level of combination between physicomachanical properties and decorative quality, they are expected to replace the traditional ceramic floor tiles completely in the next few years.

The physical and mechanical properties of porcelain bodies have been studied extensively for almost a century. During this period three theories have been presented to explain the strength of porcelains. These are the “Mullite hypothesis” (Carty and Senapati, 1998), the “dispersion strengthening hypothesis” and the “Matrix reinforcement hypothesis”. The mullite hypothesis suggests that the physical and mechanical properties of porcelain ceramic solely depends on the felt-like interlocking of fine mullite needles. Specifically, the higher the mullite content and the higher the interlocking of the mullite needles, the higher is the mechanical properties (Ece and Nakagawa, 2002). Hence, the mechanical properties of porcelain depends on the factors that affect the amount and size of mullite needles like the firing temperature (Branga and Bargmann, 2003).

On the other hand, the dispersion strengthening hypothesis states that dispersed particles in the vitreous phase of a porcelain body, such as quartz and mullite crystals, in the glassy phase of a porcelain body limit the size of Griffith flaws resulting in increased strength. The concept of the matrix reinforcement hypothesis concerns with the development of compressive stresses in the vitreous phase as a result of the different thermal expansion coefficients of dispersed particles or crystalline phases (usually quartz) and the surrounding vitreous phase. The larger these stresses are, the higher is the strength of the porcelain bodies. The phenomenon is known as the pre-stressing effect.

Although, it is suggested that a universal theory of strength in porcelain ceramic should account for all the above mechanisms of strengthening, there is abundant experimental evidence that residual quartz has deleterious effect on the physical and mechanical properties of porcelain ceramic specifically, mostly reports

that support the mullite hypothesis or the dispersion strengthening hypothesis claim that the presence of residual quartz in fired bodies is harmful to the porcelain strength due to the α - β transformation of quartz crystals during cooling (Stathis, 2008). Additionally, higher strength can be obtained by the replacement of quartz by sillimanite sand, alumina (Das and Dana, 2003), kyanite or mullite, rice husk ash, sericitic pyrophyllite or low expansion porcelain powder. The use of combination of RHA and POFA to substitute quartz has not been reported. Using RHA and POFA for the fabrication of porcelain is expected to improve some of the mechanical properties of porcelain ceramic tiles and reduce some of the problems they cause to the environment. Moreover, the use of RHA and POFA to replace quartz is expected to have effects on sintering temperature, mould pressure and soaking time.

A simultaneous investigation of parameters such as optimum composition of RHA and POFA content, optimum sintering temperature, optimum mould pressure, and optimum soaking time would help in the direction of understanding the mechanisms controlling porcelain's strength and improving its mechanical properties.

1.2 Problem statement

Quartz grains embedded in the porcelain glassy matrix have a deleterious effect on the mechanical strength mainly because of its transformation during cooling (Maity and Sarkar, 1996) which results in the development of stresses which initiate fracture (Carty and Senapati, 1998). The thermo-mechanical properties of whiteware bodies change greatly during the reconstructive and the displacive transformation of free silica due to change in volume (Prasad *et al.*, 2001).

Several researchers tried to improve the mechanical properties of porcelain ceramics by replacing quartz with other materials viz; sericitic pyrophyllite, kyanite, bauxite, sillimanite sand, alumina, RHA, silica fume and fly ash. Although the alumina in different forms has a favourable influence on the mechanical properties of white-ware due to the formation of primary mullite, it lowers the recrystallization of secondary mullite due to an increase in the viscosity of the glassy phase. On the other hand, Schuller (1964), showed that silica-rich glass favours recrystallization of mullite at low temperature and its dissolution at high temperature. Some improvements in the mechanical properties were also observed by several authors

(Kingery, 1986; Maity and Sarkar *et al.*, 1996), through the reduction of the particle size of quartz and non-plastic materials. Tomizaki (1995) reported that dissolved quartz in the glassy phase and cristobalite phase precipitation has a deleterious effect on the mechanical properties of porcelain ceramic. The use of RHA and POFA simultaneously to replace quartz in porcelain ceramic has not been presented. Additionally, replacing quartz with RHA and POFA is expected to have impact on the parameters such sintering temperature, mould pressure and soaking time. Moreover, determining the parameters such as optimum composition of RHA and POFA content, optimum sintering temperature, optimum mould pressure, and optimum soaking time would help in the direction of understanding the mechanisms controlling porcelain's strength and improving its mechanical properties.

Rice Husk (RH) is an agricultural residue abundantly available in rice producing countries. Globally, approximately 690 million tons of RH is produced each year. Therefore, total global ash production could be as high as 134 million tons per year. In Malaysia, the RH produced annually amounts to more than 2.5 million tons. In Brazil, for example, 2.5 million tons of RH is generated each year. In Thailand more than 500 thousand tonnes per year of RH is produced. Rice husk ash (RHA) is produced as a result of burning of RH by plants to generate electricity. POFA is a by-product from biomass thermal power plants where palm oil residues are burned to generate electricity. Malaysia is one of the largest producer of palm oil with around 41% of the total world supply in years 2009–2010. Since palm oil is one of the major raw materials used to produce bio-diesel, it is likely that the production of POFA will increase every year. An extensive search of the literature highlighted many uses of RHA. Two main industrial uses were identified: as an insulator in the steel industry and as a pozzolanic material in the cement industry.

Even though these are being used by steel and cement industries, very little of these ashes produced is actually used. While some of it serves as low-value material for backfill or fertilizers, most of the RHA and POFA are posed as waste in landfills, causing environmental and other problems. Within recent decades, the emission of these into the ecosystem has attracted huge criticisms and complaints, mainly associated with its persistent, carcinogenic and bio-accumulative effects, resulting in silicosis syndrome, fatigue, shortness of breath, loss of appetite (respiratory failure) and even death. Another alternative means to contribute towards solving the problem has to be looked upon. Therefore, these ashes (RHA and POFA) can be used to

substitute quartz in the production of porcelain ceramic tiles. The porcelain industries make use of natural resources for their production. Increasing world population and life demand are continuously raising the price of raw materials and reducing the natural resources; for these reasons this study is concentrated to use agric-waste materials as potential alternative in the porcelain industry. An investigation into the parameters such as temperature, mould pressure and soaking time would help towards the understanding of mechanical properties of porcelain ceramic tile.

Therefore, the present study wishes to study the mechanical properties of ceramics tiles by replacement of quartz by RHA and POFA in order to help towards sustaining the natural resources, reduce the environmental hazards caused by the ashes and to possibly add value to some of the properties of porcelain ceramic tiles.

1.3 Objectives of the study

The aim of the research is to study the effects of the replacement of RHA and POFA on properties of porcelain ceramics. In order to achieve that, four objectives were designed which are as follows:

- (i) To determine the effects of the replacement of quartz by RHA, POFA and the combination of RHA and POFA on the mechanical and physicaln properties of porcelain ceramics. Such as following:
 - (a) Mechanical properties which include, Vickers hardness, bending strength and compressive strength.
 - (b) Physical properties, which include volume shrinkage, percentage of porosity, bulk density and microstructure.
- (ii) To determine the optimum paramaters such as sintering temperature, mould pressure, soaking time with respect to the physical and mmechanical properties.

1.4 Scope of the study

In order to realise the objectives of the study to be successfully and reasonably implemented, the following scope of works have been derived.

- (i) Standard porcelain ceramic composition was adopted: Kaolin 50 wt%, feldspar 25 wt%, quartz 25 wt% (quartz was progressively replaced by RHA and POFA).
- (ii) In order to determine the optimum temperature, the temperature was varied within this range: 1000 °C, 1100 °C, 1200 °C and 1300 °C.
- (iii) The samples were produced at different mould pressures: 31 MPa, 61 MPa, 91 MPa and 121 MPa.
- (iv) The soaking time was varied from 1 hour, 2 hours and 3 hours in order to establish in order to determine the best soaking time.
- (v) Conducting the experiment to investigate and evaluate the following responses;
 - a. Volume shrinkage using (Vernier Calliper)
 - b. Percentage of porosity using (Mettler Teldo) (XS-64)
 - c. Bulk density using (Mettler Teldo) (XS-64)
 - d. Vickers hardness using (Shimadzu) (HVM-2TE)
 - e. Bending strength using (Shimadzu Autograph) (SPL-10KN)
 - f. Compressive strength using (Shimadzu Autograph) (SPL-10KN)

CHAPTER 2

LITERATURE REVIEW

2.1 Introduction on porcelain ceramic tile

Porcelain ceramic tile is a highly vitrified ceramic material produced from a body formulated by mixtures of kaolin, quartz and feldspar. The kaolin $[Al_2Si_2O_5(OH)_4]$, gives plasticity to the ceramic mixture; flint or quartz (SiO_2), maintains the shape of the formed article during sintering; and feldspar $[(K,Na)_2O \cdot Al_2O_3 \cdot 6H_2O]$, serves as flux. These three constituents place porcelain in the phase system $[(K, Na)_2O-Al_2O_3-SiO_2]$ in terms of oxide constituents, hence the term triaxial porcelain ceramic tiles (Buchanan 1991 and Olupot, 2006). The main phase composition of a porcelain body is constituted by a heterogeneous glassy matrix and needle shaped mullite crystals together with some quartz grains and closed irregular shaped pores. Mullite crystals, which are derived from the solid-state decomposition of the clay reacting with feldspar, are endowed with excellent mechanical, creep, thermal and chemical properties. Because of the complex interplay between raw materials, processing routes and the kinetics of the firing process, porcelains represent some of the most complicated ceramic systems (Lopez, 2011).

2.1.1 Raw materials of porcelain

The basic raw materials for porcelains are kaolin (50%), feldspar (25%) and quartz (25%). The kaolin fraction helps in forming, providing plasticity and dry mechanical strength during processing and forming mullite and vitreous phase during firing. The feldspars develop a liquid phase at low temperatures and assist the sintering process, allowing a virtually zero (<0.5%) open porosity and a low level of closed porosity

(<10%). The quartz promotes thermal and dimensional stability (De Noni *et al.*, 2010). These materials are also used in the production of various whiteware products. The distinguishing factor in the properties of different porcelain products are brought about by variations in the proportion of these materials, the processing and the firing schedule adopted. For porcelain, the quest over the period of time has been to increase mechanical strength, and to reduce the production costs. In most efforts to increase strength, emphasis has been placed on minimization of quartz in the porcelain formula because of the β to α phase inversion of quartz which occurs at 573 °C during cooling. The inversion results into decrease of quartz particle volume and may lead to cracks in the body. So far, there are reports of improvements in the mechanical properties by reducing the use of quartz. These include replacements of quartz with kyanite (Schroeder, 1978), Al_2O_3 (Kobayashi *et al.*, 1987 and Das and Dana 2003), RHA (Prasad *et al.*, 2001, Kurama 2008; Haslinawati *et al.*, 2009), sillimanite sand (Maity and Sarkar, 1996), fly ash (Dana *et al.*, 2004), partial replacement of feldspar and quartz by fly ash and blast furnace slag (Dana *et al.*, 2005), silica fume (Prasad *et al.*, 2002), with a mixture of RHA and silica fume (Prasad *et al.*, 2003). In this context, it can also be mentioned that an attempt to substitute part of quartz with fired porcelain by Stathis *et al.*, (2004) did not result in a positive effect on the bending strength.

Other modifications on the triaxial porcelain system, which have proven successful include, replacement of clay with aluminous cement (Tai *et al.*, 2002), substitution of feldspar with nepheline syenite (Esposito *et al.*, 2005), use of soda feldspar in preference to potash feldspar (Das and Dana, 2003), partial substitution of feldspar by blast furnace slag (Dana and Das, 2004), use of recycled glass powder to replace feldspar to reduce firing temperature (Bragança and Bergmann, 2004), the use of RHA to replace quartz (Prasad *et al.*, 2001, Kurama 2008; Haslinawati *et al.*, 2009). On the other hand, there is evidence that under optimized conditions of firing and for a particle size of 10-30 μm (Norton, 1970; Ece and Nakagawa, 2002; Bragança and Bergmann, 2003), quartz has a beneficial effect on the strength of porcelain, in conformity with the pre-stressing theory. However, the $\alpha \rightarrow \beta$ phase transformation of quartz crystals takes place at ~ 573 °C during the heating-cooling process and to the relaxation of micro-stresses originated between quartz grains and the surrounding glassy phase by the differences in their thermal expansion coefficients (Singer and Singer, 1971). Similarly, $\beta - \alpha$ cristobalite inversion occurs

at a temperature of 225 °C - 250 °C similar to the quartz inversion, but produces larger volumetric change of approximately 5% (Lundin, 1964). For small particle sizes, the dissolution is more rapid leaving less quartz crystals in the glass and hence yielding a low pre-stress and low strength of the material. For large particle sizes an interconnected matrix with favorable crack path is formed leading to low strength (Carty and Senapati, 1998). Hence, quartz grain size affects bending strength in two ways, that is, directly through the induction of compressive stresses to the vitreous phase and indirectly through the development of a favourable microstructure (Stathis *et al.*, 2004).

2.1.2 Strength consideration

The great interest in strength of porcelain for application and the wide research on the porcelain system has resulted in three major hypotheses describing the strength properties of porcelain formulations. These were described by Carty and Senapati, (1998) as the mullite hypothesis, the matrix reinforcement hypothesis and the dispersion strengthening hypothesis, respectively. The mullite hypothesis suggests that porcelain strength depends on the interlocking of fine mullite needles. Specifically, the higher the mullite content and the higher the interlocking of the mullite needles, the higher is the strength. Hence, the strength of porcelain depends on the factors that affect the amount and size of mullite needles, like the firing temperature and composition of alumina and silica in the raw materials.

The matrix reinforcement hypothesis concerns the development of compressive stresses in the vitreous phase as a result of the different thermal expansion coefficients of dispersed particles, or crystalline phases, and the surrounding vitreous phase. The larger these stresses are, the higher is the strength of the porcelain. This phenomenon is known as the pre-stressing effect. The dispersion strengthening hypothesis, on the other hand, states that dispersed particles in the vitreous phase of a porcelain body, such as quartz and mullite crystals in the glassy phase, limit the size of Griffith flaws resulting in increased strength.

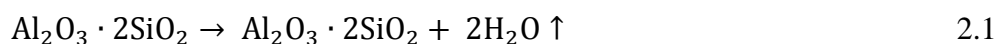
There is evidence supporting each of these hypotheses (Maity and Sarkar, 1996; Stathis *et al.*, 2004; Islam *et al.*, 2004). Carty and Senapati (1998) concluded that the typical strength controlling factors in multiphase polycrystalline ceramics are

thermal coefficients of the phases, elastic properties of the phases, volume fraction of different phases, particle size of the crystalline phases and phase transformations. Islam *et al.* (2004) concludes that the best mechanical properties can be achieved by high mullite and quartz content with low amount of the glassy phase and in the absence of micro cracks. However, a high amount of SiO₂ leads to a high amount of the glassy phase which is detrimental to the development of high mechanical strength.

2.1.3 Sintering of porcelain

During firing process, sequence of intercrystalline (regarding a single crystalline/amorphous phase) and extra crystalline (interaction of a crystalline/amorphous phase with one another) take place. Temperature, time, and atmosphere in the furnace affect chemical reactions and microstructural development in the porcelain ceramic tiles and, consequently, are important in the fired properties of porcelain. Fast firing of porcelain has gained wide recognition and application in the whiteware industry (Manfredini and Pennisi, 1995) reducing production costs by efficient use of energy in the firing process. The fast firing of porcelain requires the knowledge of chemical reactions occurring during the process and of microstructural development. Ignoring the removal of non chemically bound species, such as water and organics the basic reaction steps can be outlined as follows:

- (i) The loss of weight when kaolin is fired to temperatures exceeding about 450 °C to 550 °C under normal atmospheric conditions is commonly ascribed to “dehydration” and the water involved in the reaction is designated “structural water.” Neither term is correct, as the crystal lattice loses hydroxyl groups. The process is better described as “dehydroxylation” and it can be represented chemically by the equation.



The mechanism is most probably one of proton migration so that if two protons momentarily find themselves associated with the same oxygen ion, there is a probability that a water molecule will be formed and will detach itself. The temperature of occurrence and the exhibition of thermal events of

kaolinite generally depend upon number of variables. For example, (a) origin of kaolinite and its nature of crystallinity, size distribution and its impurities content. (b) DTA equipment and its sample holder, thermocouple, sensitivity, furnace and its atmosphere. (c) Operating conditions heating rate, sample size, packing, etc (Tarvornpanich *et al.*, 2008).

- (ii) The $\alpha \rightarrow \beta$ phase transformation of quartz crystals takes place at ~ 573 °C during the heating-cooling process and to the relaxation of micro-stresses originated between quartz grains and the surrounding glassy phase by the differences in their thermal expansion coefficients ($\alpha \sim 23 \times 10^{-6}$ °C⁻¹ for quartz and $\alpha \sim 3 \times 10^{-6}$ °C⁻¹ for the glassy phases) in the 20 °C – 750 °C temperature interval (Tarvornpanich *et al.*, 2008).
- (iii) Sanidine, the homogeneous, high-temperature, mixed-alkali feldspar, forms within 700 °C -1000 °C (Martín-Márquez *et al.*, 2010a). The formation temperature apparently is dependent on the sodium: potassium ratio.
- (iv) Metakaolin transforms to a spinel-type structure and amorphous free silica at -950 °C -1000 °C (Sonuparlak, 1987).
- (v) The amorphous silica liberated during the metakaolin decomposition is highly reactive, possibly assisting eutectic melt formation at 990 °C, as suggested by Ece and Nakagawa (2002). Carty and Senapati (1998) suggests instead that amorphous silica transforms directly to cristoballite at 1050 °C, but the general lack of cristoballite in modern commercial porcelain ceramics suggests that the former scenario is more plausible.
- (vi) Potassium feldspar melts at the temperature of 990 °C but sodium feldspar melts at 1050 °C. The lower liquid formation is beneficial to the reduction of the porcelain firing temperature. The presence of feldspar can reduce the liquid formation by as around 60 °C (Pérez *et al.*, 2012).
- (vii) Primary and secondary mullite formation takes place at a temperature of 1075 °C (Carty and Senapati 1998). Some studies however, indicates that the stable form of aluminosilicates is formed at a higher temperature (Carty and Senapati, 1998).
- (viii) At a temperature of 1200 °C, SiO₂-quartz dissolution ends, and the melt becomes saturated with the silica dissolution. Quartz-to-cristoballite transformation begins.

- (ix) At 1230 °C feldspar has totally decomposed and the body is just comprised simply of mullite crystals, quartz grains and a glassy phase (Rincón, 1992).
- (x) Pyroplastic deformation begins to take place as the porcelain body begins to cool, relaxation also starts within the glass phase to prevent the development of residual stresses until glass transition temperature is reached. As the body cools below the glass transition temperature, residual stresses are developed because of thermal expansion mismatch between the glass and the included crystalline phases (i.e., mullite and quartz, and in some cases, alumina and cristoballite).
- (xi) On cooling, quartz inversion takes place at temperature of 573 °C these results in a decrease in volume of the body by about 2 % (Carty and Senapati, 1998).
- (xii) $\beta - \alpha$ cristoballite inversion occurs at a temperature of 225 °C -250 °C similar to the quartz inversion, but produces larger volumetric change of approximately 5 % (Carty and Senapati, 1998).

2.1.4 Sintering stages

Sintering is known as a process of creating objects from powders or particles. The basic mechanism is atomic diffusion. Atomic diffusion occurs much faster at higher temperature. Few parameters are known to affect sintering such as type of materials, particle sizes, sintering atmosphere, temperature, time and heating rate (Rahaman, 2003).

There are 3 stages during sintering; starting, intermediate and finish. Figure 2.1 shows the respective stages. During adhesion stage the particles comes into contact with each other but do not form any bond. At starting stage, there is a rapid growth of the interparticle neck between the particles. At intermediate stage the pore structure becomes smooth (reach equilibrium shape) and develops interconnected particles. The intermediate stage usually covers the major part of the sintering process. Particles start to form grain boundaries. At the final stage, the densification process is stopped and the pores become spherical and separated.

Sintering occurs by diffusion of atoms through the microstructure. This diffusion is caused by a gradient of chemical potential-atoms that move from an

area of higher chemical potential to an area of lower chemical potential. The different paths that the atoms take to get from one spot to another are known as the sintering mechanisms. The six common mechanisms are:

- (i) Surface diffusion – diffusion of atoms along the surface of a particle
- (ii) Vapor transport – evaporation of atoms which condense on a different surface
- (iii) Lattice diffusion from surface – atoms from surface diffuse through lattice
- (iv) Lattice diffusion from grain boundary – atom from grain boundary diffuses through lattice
- (v) Grain boundary diffusion – atoms diffuse along grain boundary
- (vi) Plastic deformation – dislocation motion causes flow of matter

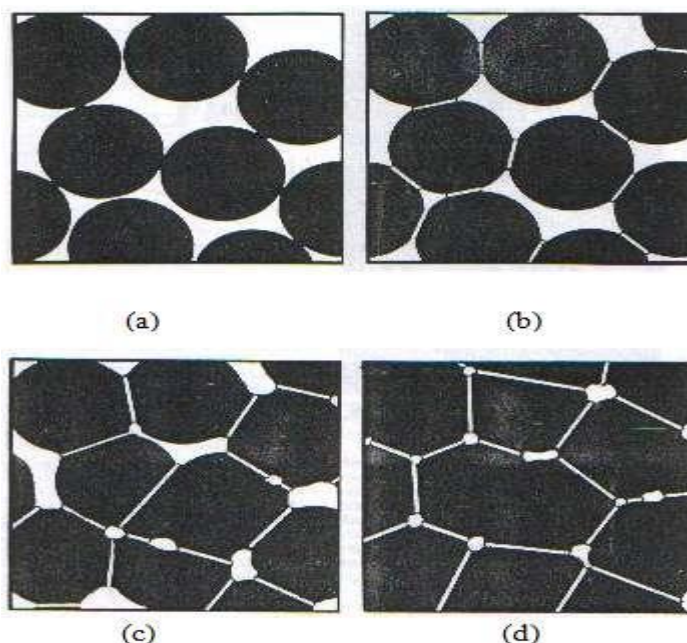


Figure 2.1: Stages of sintering (a) free particles, (b) necking between particles, (c) formation of grain boundary, and (d) densification process and pores elimination (Randal, 1991)

The firing of porcelain promotes physico-chemical reactions responsible for the final properties of the ceramic products. In this process, it must be considered the kinetic limitations, the development of the phases, and the complexities of the microstructure. Generally, all the steps, since raw material preparation, drying conditions and firing cycle are going to have a strong influence in the product qualities. The firing cycle influence is related to the kind of furnace, firing

atmosphere, maximum temperature mould pressure and soaking time. All these parameters are related to quality and cost of the products.

The work of Mattyasovszky-Zsonay (1957) is very conclusive with respect to porcelain mechanical strength. Mattyasovszky-Zsonay has recommended a particle diameter of quartz of 10–30 μm and shown the influence of quartz. He disregarded the effect of mullite and explained the prestress theory. Schuller (1979) has made an analogy between quartz content and particle size explaining mechanical strength as a consequence of radial and tangential stress. Schuller found that a variation in strength occurred with a variation in quartz content. He also highlighted that the best diameter of quartz is between 15 and 30 μm . Carty and Senapati (1998) examined three hypothesis: (1) mullite, (2) matrix reinforcement and (3) dispersion strengthening mechanism. They concluded that these three factors have an influence but the principal factor depends on the microstructure. The intrinsic flaw can be either a simple pore in a sample containing a glassy phase, or a pre existing crack in a sample that does not contain a glassy phase. This is due to the presence of quartz and cristobalite. Kobayashi *et al.* (1992) found a high bending strength body containing a large amount of porosity. This body presented small pores distributed uniformly within the microstructure. The apparent porosity was zero although a high relative density was not obtained. Bradt as reported by Kobayashi *et al.*, (1992) based his explanation of the effect of quartz on the strength on Linear Fracture Mechanics. He found a K_{IC} value of $1.3 \text{ MPa m}^{1/2}$ for a body containing 10–30 μm quartz particle size.

The influence of the flux used in the fast firing of porcelain was investigated by Mortel and Pham-Gia (1981). The author compared the properties obtained in porcelains composed of K-feldspar or Na-feldspar and concluded that they are strongly influenced by the viscosity of the glass phase during firing. The glass phase depends on the kind of the flux used in the batch. Lee and Iqbal (2001) discovered forms of mullite occurring in typical porcelains. According to them, they are: (1) Primary mullite from decomposition of pure clay. (2) Secondary mullite from reaction of feldspar and clay and feldspar, clay and quartz. Additionally, in aluminous porcelains (3) Tertiary mullite may precipitate from alumina-rich liquid obtained by dissolution of alumina filler. They stressed the the size and shape of mullite crystals is to large extent controlled by the fluidity of the local liquid matrix from which they precipitate, and in which they grow, which itself is a function of its temperature and

composition. The composition of this local liquid was determined by the extent of mixing of the porcelain raw materials and the role of the flux is critical.

Braganca *et al.* (2004) investigated the mechanical properties of porcelain. They reported the optimum sintering temperature for the porcelain studied was 1340 °C using a heating rate of 150 C/h and a 30 min soaking time. At this temperature the modulus of rupture and bulk density were at a maximum. The authors recorded the technical parameters are summarized such as water absorption: 0.34%, apparent porosity: 0.84%, bulk density: 2.48 g/cm³ linear shrinkage: 12.2% modulus of rupture: 46 MPa. Their analysis of the technical data showed that the modulus of rupture and the bulk density were related. The authors added that the maximum strength is a result of decrease in porosity and internal flaws. Samples fired at temperatures below the ideal (1340 °C) showed open porosity. Above this, according to them, temperature an increasing in closed porosity occurred due to oxygen releasing and bloating. They further explained that two types of porosity caused a decrease in sample strength. For the ideal firing temperature (1340 °C) they found out that the fracture toughness is $K_{IC}=1.6 \text{ MPa m}^{1/2}$, the fracture energy =16.4 J/m² and crack length $c=200 \text{ mm}$. These according the author parameters are good values for a fine ceramic. On the microstructural analysis Braganca *et al.* (2004) revealed that the ideal firing temperature occurs when the glassy phase covers the entire sample surface with sufficient time to react with crystalline phases. Higher temperatures were limited by the porosity increase. This porosity is a result of oxygen released from Fe₂O₃ decomposition and gas expansion in the pores.

Stathis (2004) asserts that filler grain size has severe impact on the mechanical and physical properties of porcelain compared to the impact of the other three factors, namely quartz content in the filler, firing temperature and soaking time that were tested. Thus, optimization efforts should be focused on this factor. According to Stathis (2004), bending strength is affected by quartz grain size in two ways, directly through the induction of compressive stresses to the vitreous phase and indirectly through the development of a favorable microstructure. He stressed that both the parameters depend strongly on the particle distribution of quartz grains. He recorded the optimum quartz grain size is 5–20 µm which gives the maximum bending strength. However, he noticed that the use of coarser grain sizes results in reduced bending strength due to the development of a detrimental microstructure for the mechanical properties.

The microstructure of the samples is very porous and characterized by large, irregular pores connected to each other. On the other hand, using finer quartz grains results in low bending strength due to limited pre-stressing effect. Controlling quartz grain size in the optimum range bending strength is increased by 20–30% compared to the reference porcelain. The results are consistent with the matrix reinforcement theory. He however, concludes that the beneficial influence of mullite content on bending strength is not confirmed. In addition, they concluded that replacing part of quartz content with fired porcelain did not result in a positive effect on bending strength.

In a study carried out by Tucci *et al.* (2004), investigated, the possibility of replacing a percentage of the sodium feldspar with soda-lime scrap-glass in a standard porcelain ceramic stoneware tile mix. According to them the replacement of 10 wt.% of the sodium feldspar with the same amount of soda-lime scrap-glass causes the following remarkable effects such as: decrease in firing temperature, an increase in mechanical resistance. The authors emphasized the importance of the possibility of improving the characteristics of a product, and at the same time finding a use for a waste material, the availability of which is increasing.

Romero *et al.* (2006) carried out a research on the crystallisation kinetic and growth mechanism of mullite crystals in a standard porcelain stoneware powder of composition 50% kaolinitic clay, 40% feldspar and 10% quartz for tiles production have been investigate by DTA method. From the experimental results, the authors were conclusive on the following. (1) The temperature of mullite crystallisation in the porcelain stoneware powder was around 985 °C. (2) The activation energies of mullite crystallisation in porcelain stoneware calculated by both isothermal (Ligero method) and non-isothermal (Kissinger method) treatments are 599 and 622 kJ mol⁻¹, respectively. (3) The values of the growth morphology parameters n and m are found to be $n = m \approx 1.5$ indicating that bulk nucleation is the dominant mechanism in mullite crystallisation and a three-dimensional growth of mullite crystals with polyhedron-like morphology controlled by diffusion from a constant number of nuclei.

The results obtained by Tucci *et al.* (2007), pointed out the increase of crack resistance, registered for the modified body mixes, was attributed to the presence of the alumina particles. Since, the fracture toughness of the particles is higher than that of the glassy matrix, the authors stated that it is justified to believe that different

toughening mechanisms, deflection of the crack path and crack stopping, influenced crack propagation. Besides, they observed that the presence of spodumene, due to its capability to develop a low viscosity liquid phase, improves the sintering performances of the modified products, reduces porosity and favours the crystallisation of rather elongated needle like mullite.

Kemseu *et al.* 2007 produces soft and hard porcelain with excellent technical characteristics from two different china clays from Cameroon and carried out an investigation into them. From the results obtained in their work, he concluded that the two China clays from Cameroon are suitable as clay for porcelain bodies. According to Kemseu *et al.* (2007), the properties of the final products show that: Soft porcelain with low clay content and higher proportion of fluxing agent can be produced in the range of temperature of 1200–1225 °C with average density of 2.4 g/cm³, water absorption less than 0.1% and flexural strength of 149 MPa. Hard porcelain bodies with higher clay content and relatively low proportion of fluxing agent can be produced in the range of temperature of 1325 °C –1350 °C and flexural strength of 167 MPa. He added therefore, that the use of China clays with TiO₂ and FeO₂ content permits a decrease of 25 °C in firing temperature. This should reduce production costs which makes its utilisation very attractive, especially for tiles where the white colour is not required.

Ece and Nakagawa (2002) have shown that a maximum bending strength for a 10–30 mm quartz grain size occurs after firing at 1300–1350 °C. They explained that fractures initiating from flaws were micro-cracks around quartz grains acting as links between closed pores.

Transmission Electron Microscope (TEM) and acoustic emission were used by Ohya and Takahashi (1999) in order to analyze the microstructure of a porcelain body. They presented TEM micrographs showing peripheral cracks around quartz. They pointed out that these cracks are a consequence of quartz and matrix expansion mismatch during cooling from temperatures below 1000 °C.

Quartz grains embedded in the porcelain glassy matrix have a deleterious effect on the mechanical strength mainly because of its transformation during cooling (Schroeder, 1978; Mattyasovszky-Zsolnay, 1957; Mortel 1977) which results in the development of stresses which initiate fracture (Zhang, 1999). The thermo-mechanical properties of whiteware bodies change greatly during the reconstructive

and the displacive transformation of free silica due to change in volume, which was reviewed in detail by Kingery (1960).

Several investigators (Maity and Sarkar, 1996; Prasad *et al.*, 2001; Prasad *et al.*, 2002; Derevyagina *et al.*, 1980, Das and Dana, 2004; kalapathy 2007; Haslinawati 2009) tried to improve the mechanical properties of whiteware bodies by replacing quartz with other materials viz; sericitic pyrophyllite, kyanite, bauxite, sillimanite sand alumina, fly ash and RHA. Although the alumina in different forms has a favourable influence on the mechanical properties of whiteware due to the formation of primary mullite, it lowers the recrystallisation of secondary mullite due to an increase in the viscosity of the glassy phase. On the other hand, only three researchers reported the use RHA to substitute quartz (Kalapathy 2000: Prasad *et al.*, 2001; Kurama 2008; Haslinawati, 2009) in the porcelain ceramic tile.

Maity and Sarkar (1996) studied the effect of sillimanite sand as a replacement for quartz and alumina/cordierite glass-ceramic for feldspar was studied. Compositional variations were due to the gradual incorporation of alumina in place of cordierite glass-ceramic was observed. Increased replacement of cordierite glass-ceramic by alumina (20%) increased the flexural strength by 100%, giving a value of 195 MPa was noted. The authors however, discovered that elastic modulus, micro hardness and fracture toughness also showed sharp increases compared with values for conventional triaxial whiteware compositions. They concluded that improvement in mechanical properties was attributed to the presence of sillimanite and alumina particles present as fracture-resistant dispersions in a viscous glassy matrix. Increased fracture behaviour is due to minimization of the glassy phase and limiting the size of Griffith's flaws.

In a previous study Prasad *et al.* (2001), studied the effects of the substitution of quartz by RHA in whiteware ceramic. The authors observed that the progressive substitution of quartz by RHA in a conventional whiteware composition resulted in an early vitrification of the mixes. A reduction in the maturing temperature of about 50 °C to 100 °C was noticed in the body mixes containing RHA compared to the reference body. They further explained that the increase in the fired strength and the substantial decrease in per cent thermal expansion of the body mixes containing RHA are attributed to the sharp decrease in the quartz content and also to the increase in the content of the glassy phase. However, they reported that the content of mullite appeared to be unaffected due to the addition of RHA in the compositions.

The reduction in the vitrification temperature of the mixes also contribute significantly to the economical production of whitewares.

In a study carried out by Chen *et al.* (2000), demonstrates that mullite can be prepared by reaction sintering kaolinite and alumina. The advantage of their process is its economic feasibility. The disadvantage of it, was its relatively high sintering temperature, low density and consequently low strength. The authors observed the alumina particles are inert to kaolinite until 1200 °C. According to the study the reaction between alumina and the glass phase to form mullite starts from 1300°C. They stressed that the sintering temperature of the (kaolin+alumina) powder compacts has therefore to be higher than 1300 °C. Nevertheless, the authors pointed out that the disadvantage can be coped with by adding flux such as feldspar into kaolin. The reaction between kaolinite and alumina was accompanied with a shrinkage. The study also revealed the the presence of glassy phase facilitates the formation of large holes. Fully dense mullite specimens are thus difficult to prepare by using the process employed in the present study. The strength of the specimens was therefore low. However, the toughness of the specimen increases with the increase of alumina content.

Braganc *et al.* (2002) produced porcelain with excellent technical characteristic which had similar properties to a traditional porcelain by substituting quartz with glass powder. From the results they obtained they concluded that the use of recycled soda–lime glass powder as a fluxing agent to replace feldspar in porcelain was viable. The appropriate firing temperature for glass powder porcelain was 1240 °C and for traditional porcelain was 1340 °C. Therefore they asserted, that the use of glass powder permitted a decrease of 100 °C in firing temperature to be made. The authors added that it would mean a reduction in production costs which will make the utilisation of glass powder porcelain very attractive. They found out that the firing curve (water absorption and linear shrinkage and firing temperature) shows that glass powder porcelain has a behaviour typical of a strong flux.

Glass powder porcelain has an advantageously low firing temperature, but a shorter sintering range compared to traditional porcelain. The authors added that after firing at the appropriate temperature the modulus of rupture and bulk density were higher for traditional porcelain by. They however, noted that because of a high MOR (38 MPa) and low water absorption (0.39%) glass powder porcelain attained the technical specifications of a porcelain stoneware. Similarly, the authors

discovered that the microstructural analysis revealed that the ideal firing temperature occurred when the glassy phase covered the entire sample surface and had a sufficient time to react with the crystalline phases. They however stresses that at higher temperatures were deleterious to the properties of porcelain due to an increase in porosity. The porosity according to them was due to the release of oxygen from the decomposition of Fe_2O_3 and gas expansion within the pores. The higher amount of closed porosity in glass powder porcelain porcelain explains why this porcelain did not attain a higher bulk density.

In a research conducted by Prasad *et al.* (2002), where they substituted quartz with silica fume found that the incorporation of silica fume in place of quartz in whiteware bodies lowers the vitrification temperature. They noticed a reduction in the maturing temperature of about 50–100 °C was noticed in the body mixes containing 5–25 wt.% of silica fume compare to that of the reference body. They also discovered that increase in the fired strength about 10% with 10 wt.% silica fume and decrease in the thermal expansion (5.95%) are attributed to the sharp decrease in the content of quartz and also to the increase in the content of the glassy phase. However, according to them the content of mullite appeared to be unaffected due to addition of silica fume in the compositions but with a change in the size of mullite crystals and its orientation as observed in the micrographs. They concluded that reduction in the vitrification temperature of the body mix containing 25 wt.% silica fume with a substantial decrease in percentage of thermal expansion (~34%) was observed which would contribute significantly to the improvement of the economical production of whitewares.

Das and Dana (2003) investigated the differences in densification behaviour of K- and Na-Feldspar-containing porcelain bodies. They reported that the sequence of chemical reactions during thermal heating of potash- and soda-feldspar-containing triaxial porcelain compositions using DTA–TGA technique. The authors observed that both the compositions followed similar reaction steps up to 1000 °C, beyond which feldspar forms eutectic melt and starts reacting. The difference in their densification behaviour has been studied using high temperature dilatometer. The soda-feldspar-containing composition exhibits maximum densification rate of 1171 °C compared to 1195 °C for the potash-feldspar-containing composition. A separate set of pressed samples heated in an electric furnace to temperatures of 1160–1200 °C showed almost similar densification behaviour. The soda-feldspar-containing

composition achieved higher BD (2.43 gm/cm^3), lower %WA (0.07%) and highest flexural strength (53.14 MPa) at $1200 \text{ }^\circ\text{C}$ compared to potash-feldspar-containing composition. The whiteness of potash-feldspar-containing body is poorer than soda-feldspar-containing body due to increased amount of Fe_2O_3 and TiO_2 impurities present in it.

Olgun *et al.* (2005) demonstrated that it is possible to utilize fly ash and tincal waste as alternative raw material resources for the production of the wall tile. On the basis of their results the authors reported that the use of tincal waste and fly ash in the standard wall tile composition increases the firing shrinkage. Moreover, they asserts that the combination of fly ash and tincal waste helps in controlling firing shrinkage of the tile. According to Olgun *et al.* (2005), regardless of the replacement level, introduction of fly ash and tincal waste into wall tile composition increases the firing strength compared to that of standard wall tile. The authors noted that the increases in the firing strength is more pronounced as the replacement level of tincal waste and fly ash content was increased. Firing strength of the tiles containing tincal waste is higher than that of the control tile and the tile containing fly ash. The result shows that the firing strength is directly related to the tincal waste content in the wall tile, which increases as the tincal waste content of the tile compositions is increased. Water absorption of tile decreases as the tincal waste content of the tile is increased. They concluded that tiles containing up to 10 wt.% of fly ash of and 5 wt.% of tincal waste into wall tile body show a good mineralogical and rheological compatibility with the pure wall tile product.

Dana and Das (2004) investigated the effects of the substitution of quartz by fly ash in a normal porcelain ceramic body. The authors stated that results in increase in the linear shrinkage, bulk density and decreases the apparent porosity in the entire temperature range of heating ($1150\text{--}1300 \text{ }^\circ\text{C}$). This, according to them was be due to the formation of low viscosity glass which flows easily and helps in better liquid phase sintering. They added that the mullite content increases with the addition of fly ash in place of quartz and thereby improves the flexural strength significantly. They further explained that, residual quartz content decreases with fly ash addition. They also observed that the scanning electron micrographs taken on the $1300 \text{ }^\circ\text{C}$ heated samples reveal the presence of α -quartz and secondary mullite embedded in the glassy matrix in general. Better interlocking and uniform distribution of

comparatively smaller sized mullite needles in the glassy matrix explain the high strength achieved.

Mukhopadhyay *et al.* (2006) discovered that the incorporation of pyrophyllite as a progressive replacement of quartz in a porcelain composition resulted in early vitrification. According this also resulted in substantial reduction in the thermal expansion due to development of interlocking mullite needles. In addition they explained that pyrophyllite reduced fired shrinkage and improved the flexural strength compared to the standard body. This was primarily due to the elimination of stresses in the structure with decreasing quartz content as well as due to presence of the feltlike interlocking of fine mullite needles in higher proportions. Mukhopadhyay *et al.* (2006) stress that mullite was found even at 1150 °C and its amount increased up to 1250 °C before decreasing at higher temperature. Beyond some optimum proportion of pyrophyllite (in this study 15%) there occur a large volume of glass formation and large elongated pores non-uniformly distributed in the microstructure which resulted in deterioration of the mechanical properties. The amount of closed pores in the specimens with pyrophyllite content beyond 15% and fired at 1300 °C was found to increase very abruptly which in turn is expected to increase the mean free fracture path per unit volume resulting in the decrease in strength.

The addition of fly ash and blast furnace slag in a traditional triaxial porcelain composition in the proportion of 1:1 and 1:2 has been studied by Dana and Das (2005). It was found to be beneficial towards improvement in mechanical strength and early vitrification at 1175 °C. Presence of microcrystalline components of quartz and mullite in fly ash and alkaline earth oxides in blast furnace slag were responsible to develop anorthite and mullite phases which ultimately improved the mechanical strength. They stressed that such type of synergistic porcelain composition may find potential applications to manufacture high strength ceramic floor tiles for industrial as well as domestic buildings. Further, part substitution of natural minerals (quartz and feldspar) by overburden industrial by-products (fly ash and blast furnace slag) reduce the cost of raw materials, thermal energy without altering the requisite physico-mechanical properties.

Furlani (2008) studied synthesis and characterization of ceramics from coal fly ash and incinerated paper mill sludge. The authors observed that materials obtained from paper mill sludge alone are fractured and not suitable for production of

monolithic ceramics. Materials obtained from coal fly ash alone can be sintered, but the control of the sintering process is difficult since green bodies shrink and melt in a restricted range of temperatures. Intermediate compositions have a progressive shrinkage and fired materials are mainly polycrystalline. Their water absorption is low and their mechanical properties are fair. More in particular, the authors concluded that the composition containing 25 wt% of coal fly ash and 75 wt% of powders from paper mill sludge show the best overall behaviour.

Martín-Márquez *et al.* (2008) study a mixture of 50% kaolinitic clay, 40% feldspar and 10% quartz composition of commercial porcelain stoneware tiles produced by a fast-firing process. They found out that all bodies show a good sintering behaviour after firing in the 1200–1300 °C range. The study revealed that the fired samples are homogeneous and free of defects such as holes, bubbles or cracks. They added that the linear shrinkage, water absorption and porosity determinations show that the sintering process in porcelain stoneware samples does not exactly proceeded by a viscous liquid phase mechanism. The authors further explained that close porosity starts to increase before open porosity totally disappears. This according to the authors behaviour is due to both mullite crystallization and quartz dissolution in the liquid phase, which originate an increase in the viscosity of liquid phase and hence, the removal of open porosity is delayed. The optimum firing temperature is achieved in the 1260–1280 °C range, when open porosity reaches a minimum value and simultaneously linear shrinkage is maximum. Firing above vitrification range results in a drastic fall of the physical properties due to forced expulsion of the entrapped gases, resulting in blisters and bloating.

Andreola *et al.* (2008) carried out a research on recycling of cathode ray tube (CRT) panel glass as fluxing agent in the porcelain stoneware tile production. The authors suggested that the ceramic sector might represent a suitable alternative to recycle this kind of waste glass as fluxing agent in the porcelain stoneware body. They explain that the addition of low viscosity panel glass has shown a positive effect on the quartz dissolution and on the formation of liquid phase, which give the possibility to reduce the amount of feldspar in the mass. Used in small amounts (up to 5 wt.%), it can replace conventional flux agents improving the densification process (linear shrinkage, water absorption, apparent density) and the mechanical properties (Young' modulus). They added that during firing CRT screen glass gets better sintering kinetic with some positive effects: lower final open and total porosity

and higher apparent density. CRT glass added up to 10 wt.% does not change the crystalline phases present and consequently the microstructure.

Yürüyen and Toplan (2009) studied the effect of waste glass additions on the sintering properties of fly ash in porcelain bodies between 1100 °C and 1200 °C in air. In their study, they selected a basic porcelain composition consisting of 50% kaolin, 30% potassium-feldspar and 25% quartz, and fly ash was used instead of quartz at the selected porcelain composition. This composition was very similar to the basic porcelain composition. The authors found out that the sintering activation energy value of the porcelain was 145 kJ/mol for a composition of 10 wt.% waste glass addition which was very close to the value of 137.618 kJ/mol as reported by Demirkıran *et al.* (2002). Replacement of potassium-feldspar with waste glass resulted in a reduced activation energy required to initiate sintering in porcelain samples. Therefore, they concluded that the densification rate could be increased. As a consequence of the lower activation energy, according to them it may be possible to produce the porcelain at 1200 °C instead of 1300–1350 °C. Moreover, they noted that it may be possible to use waste glass and fly ash instead of quartz and potassium-feldspar as raw materials in porcelain compositions.

Mostafa *et al.* (2010) uses blast furnace to substitute quartz. They revealed that the blast furnace slag can be used alone or with combination of aluminum silicate minerals to produce ceramic materials using the conventional ceramic firing process. The sintering process in kaolin–slag mixtures proceeded by a viscous liquid phase mechanism at temperatures lower than 1000 °C. Liquid phase assisted sintering and offered rapid densification kinetics. They however, noted that ceramic materials can be produced from blast furnace by low cost powder sintering route with conventional sintering process at temperatures above softening point. The authors concluded that blast furnace alone or mixed with up to 50% aluminum silicate minerals could be successfully used for production of low cost ceramic materials. Low partial substitution of blast furnace slag by kaolin (10%) increased the densification and strength at low sintering temperature.

Martín-Márquez *et al.* (2010) studied a mixture of 50% kaolinitic clay, 40% feldspar and 10% quartz as a representative composition of commercial porcelain stoneware (PSW) tiles produced via a fast-firing process. PSW samples fired in the 500–1000 °C interval show a typical underfired ceramic microstructure comprised of clay agglomerates, feldspar particles, quartz grains and a fine matrix of clay, feldspar

REFERENCES

- Abadir, M. F., Sallam, E. H., & Bakr, I. M. (2002). Preparation of porcelain tiles from Egyptian raw materials, 28, 303–310.
- Abbas, A., & Ansumali, S. (2010). Global potential of rice husk as a renewable feedstock for ethanol biofuel production. *BioEnergy Research*, 3(4), 328-334.
- Abdul Awal, A. S. M., & Warid Hussin, M. (2011). Effect of palm oil fuel ash in controlling heat of hydration of concrete. *Procedia Engineering*, 14, 2650-2657.
- Afroz, R., Hassan, M. N., & Ibrahim, N. A. (2003). Review of air pollution and health impacts in Malaysia. *Environmental Research*, 92(2), 71-77.
- Ahmad, M. H., Omar, R. C., Malek, M. A., Noor, N., & Thiruselvam, S. (2008). Compressive strength of palm oil fuel ash concrete. In *In International Conference on Construction and Building Technology (ICCBT)*.
- Ahmadi, M. A., Alidoust, O., Sadrinejad, I., & Nayeri, M. (2007). Development of mechanical properties of self compacting concrete contain rice husk ash. *International Journal of Computer, Information, and Systems Science, and Engineering*, 1(4), 259-262.
- Ahmed, A. E., & Adam, F. (2009). The benzylolation of benzene using aluminium, gallium and iron incorporated silica from rice husk ash. *Microporous and Mesoporous Materials*, 118(1), 35-43.
- Ajiwe, V. I. E., Okeke, C. A., & Akigwe, F. C. (2000). A preliminary study of manufacture of cement from rice husk ash. *Bioresource Technology*, 73(1), 37-39.
- Al-Hilli, M. F., & Al-Rasoul, K. T. (2013). Characterization of alumino-silicate glass/kaolinite composite. *Ceramics International*.
- Almeida, M. I., Almeida, N. G., Carvalho, K. L., Gonçalves, G. A. A., Silva, C. N., Santos, E. A., ... & Vargas, E. A. (2012). Co-occurrence of aflatoxins B1, B2, G1 and G2, ochratoxin A, zearalenone, deoxynivalenol, and citreoviridin in rice in Brazil. *Food Additives & Contaminants: Part A*, 29(4), 694-703.
- Altwair, N. M., Johari, M. A. M., & Hashim, S. F. S. (2011). Strength activity index and microstructural characteristics of treated palm oil fuel ash. structure, 5, 6.

- Altwair, N. M., Johari, M. A., Hashim, S. F. S., & Zeyad, A. M. (2013). Mechanical Properties of Engineered Cementitious Composite with Palm Oil Fuel Ash as a Supplementary Binder. *Advanced Materials Research*, 626, 121-125.
- Alves, H. J., Freitas, M. R., Melchiades, F. G., & Boschi, A. O. (2011). Dependence of surface porosity on the polishing depth of porcelain stoneware tiles. *Journal of the European Ceramic Society*, 31(5), 665-671.
- Amick, J. A. (1982). Purification of rice hulls as a source of solar grade silicon for solar cells. *Journal of the Electrochemical Society*, 129(4), 864-866.
- Amick, J.A. (1985). Purification of Rice Hulls as a Source of Solar Grade Silicon for Solar Cells. *Journal of Electrochemical Society*, 34, pp. 269-273.
- Amorós, J. L., Orts, M. J., García-Ten, J., Gozalbo, A., & Sánchez, E. (2007). Effect of the green porous texture on porcelain tile properties. *Journal of the European Ceramic society*, 27(5), 2295-2301.
- Amrutkar, P. P., Patil, S. B., Todarwal, A. N., Wagh, M. A., Kothawade, P. D., & Surawase, R. K. (2011). Design and evaluation of taste masked chewable dispersible tablet of lamotrigine by melt granulation. *International Journal of Drug Delivery*, 2(2).
- An, D., Guo, Y., Zou, B., Zhu, Y., & Wang, Z. (2011). A study on the consecutive preparation of silica powders and active carbon from rice husk ash. *biomass and bioenergy*, 35(3), 1227-1234.
- Andreola, F., Barbieri, L., Karamanova, E., Lancellotti, I., & Pelino, M. (2008). Recycling of CRT panel glass as fluxing agent in the porcelain stoneware tile production. *Ceramics International*, 34(5), 1289-1295.
- Armesto, L., Bahillo, A., Veijonen, K., Cabanillas, A., & Otero, J. (2002). Combustion behaviour of rice husk in a bubbling fluidised bed. *Biomass and Bioenergy*, 23(3), 171-179.
- Awal A.S. and Hussain M.W.(1997). The effectiveness of palm oil fuel ash in preventing expansion due to alkali-silica reaction. *Cement Concrete Com*, 19(4), pp. 96-105
- Awal, A. S. M. A., & Nguong, S. K. (2010). A Short-Term Investigation on High Volume Palm Oil Fuel Ash (POFA) Concrete. *Proceedings of the 35th Conferenece on our World in Concrete and Structure*, 185-192.
- Bansal, V., Ahmad, A., & Sastry, M. (2006). Fungus-mediated biotransformation of amorphous silica in rice husk to nanocrystalline silica. *Journal of the American Chemical Society*, 128(43), 14059-14066.
- Basegio, T., Haas, C., Pokorny, A., Bernardes, A. M., & Bergmann, C. P. (2006). Production of materials with alumina and ashes from incineration of chromium tanned leather shavings: environmental and technical aspects. *Journal of hazardous materials*, 137(2), 1156-1164.

- Beheri, H. H., Mohamed, K. R., & El-Bassyouni, G. T. (2012). Mechanical and microstructure of reinforced hydroxyapatite/calcium silicate nano-composites materials. *Materials & Design*.
- Bondioli, F., Andreola, F., Barbieri, L., Manfredini, T., & Ferrari, A. M. (2007). Effect of rice husk ash (RHA) in the synthesis of (Pr, Zr) SiO₄ ceramic pigment. *Journal of the European Ceramic Society*, 27(12), 3483-3488.
- Bouzidi, N., Bouzidi, A., Gaudon, P., Merabet, D., & Blanchart, P. (2013). Porcelain containing anatase and rutile nanocrystals. *Ceramics International*, 39(1), 489-495.
- Bragança, S. R., Vicenzi, J., Guerino, K., & Bergmann, C. P. (2006). Recycling of iron foundry sand and glass waste as raw material for production of whiteware. *Waste management & research*, 24(1), 60-66.
- Bragança, S.R. and Bergmann, C.P. (2003) "A View of Whitewares Mechanical strength and microstructure" *Ceramics International* 29, pp 801-806.
- Bragança, S.R. and Bergmann, C.P. (2004) "Traditional and glass powder porcelain: Technical and Microstructure analysis" *Journal of the European Ceramic Society* 24, pp 2383-2388.
- Bribiesca, S., Equihua, R., & Villaseñor, L. (1999). Photoacoustic thermal characterization of electrical porcelains: effect of alumina additions on thermal diffusivity and elastic constants. *Journal of the European Ceramic Society*, 19(11), 1979-1985.
- Brindley, G. W., & Nakahira, M. (1959). The Kaolinite-Mullite Reaction Series: I, A Survey of Outstanding Problems. *Journal of the American Ceramic Society*, 42(7), 311-314.
- Buchanan, R.C. (1991) *Ceramic Materials for Electronics* (R.C. Buchanan, Ed.) Chap. 1. Dekker, New York.
- Bui, D. D., Hu, J., & Stroeven, P. (2005). Particle size effect on the strength of rice husk ash blended gap-graded Portland cement concrete. *Cement and Concrete Composites*, 27(3), 357-366.
- Callister, D. W. And Rethwisch G.D. (2008). *Fundamentals of Materials Science and Engineering* 3rd ed. U.S.A.: John Wiley & Sons, Inc.
- Carty, W. M., & Senapati, U. (1998). Porcelain—raw materials, processing, phase evolution, and mechanical behavior. *Journal of the American Ceramic Society*, 81(1), 3-20.
- Celik, H. (2011). Effect of spray-dried powder granularity on porcelain tile properties. *Journal of Ceramic Processing Research*, 12(4), 483-487.
- Chakraverty, A., Mishra, P., & Banerjee, H. D. (1988). Investigation of combustion of raw and acid-leached rice husk for production of pure amorphous white silica. *Journal of Materials Science*, 23(1), 21-24.

- Chandara, C., Mohd Azizli, K. A., Ahmad, Z. A., Saiyid Hashim, S. F., & Sakai, E. (2012). Heat of hydration of blended cement containing treated ground palm oil fuel ash. *Construction and Building Materials*, 27(1), 78-81.
- Chandara, C., Sakai, E., Azizli, K. A. M., Ahmad, Z. A., & Hashim, S. F. S. (2010). The effect of unburned carbon in palm oil fuel ash on fluidity of cement pastes containing superplasticizer. *Construction and Building Materials*, 24(9), 1590–1593.
- Chandrasekhar, S.; Satyanarayana, K. G.; Pramada, P. N.; Raghavan, P. and Gupta, T. N. (2003). Review Processing, Properties and Application of Reactive Silica from Rice Husk – An Overview. *Journal of Materials Science*. 38: 3159-3168.
- Chatveera, B., & Lertwattanaruk, P. (2011). Durability of conventional concretes containing black rice husk ash. *Journal of environmental management*, 92(1), 59–66.
- Chaudhry, A. A., Yan, H., Gong, K., Inam, F., Viola, G., Reece, M. J., ... & Darr, J. A. (2011). High-strength nanograined and translucent hydroxyapatite monoliths via continuous hydrothermal synthesis and optimized spark plasma sintering. *Acta Biomaterialia*, 7(2), 791-799.
- Chavalparit, O. (2006a). Clean technology for the crude palm oil industry in Thailand. Wageningen University.
- Chavalparit, O., Rulkens, W. H., Mol, A. P. J., & Khaodhair, S. (2006b). Options for environmental sustainability of the crude palm oil industry in Thailand through enhancement of industrial ecosystems. *Environment, Development and Sustainability*, 8(2), 271-287.
- Chen, H., Zhao, C., & Ren, Q. (2012). Feasibility of CO₂/SO₂ uptake enhancement of calcined limestone modified with rice husk ash during pressurized carbonation. *Journal of environmental management*, 93(1), 235–44.
- Cheng, Y., Lu, M., Li, J., Su, X., Pan, S., Jiao, C., & Feng, M. (2012). Synthesis of MCM-22 zeolite using rice husk as a silica source under varying-temperature conditions. *Journal of colloid and interface science*, 369(1), 388-394.
- Chiew, Y. L., & Cheong, K. Y. (2011). A review on the synthesis of SiC from plant-based biomasses. *Materials Science and Engineering: B*, 176(13), 951-964.
- Chindaprasirt, P., & Rukzon, S. (2008). Strength, porosity and corrosion resistance of ternary blend Portland cement, rice husk ash and fly ash mortar, 22, 1601–1606.
- Chindaprasirt, P., Homwuttiwong, S., & Jaturapitakkul, C. (2007b). Strength and water permeability of concrete containing palm oil fuel ash and rice husk–bark ash. *Construction and Building Materials*, 21(7), 1492-1499.
- Chindaprasirt, P., Jaturapitakkul, C., & Rattanasak, U. (2009). Influence of fineness of rice husk ash and additives on the properties of lightweight aggregate. *Fuel*, 88(1), 158–162.

- Chindaprasirt, P., Kanchanda, P., Sathonsaowaphak, a., & Cao, H. T. (2007a). Sulfate resistance of blended cements containing fly ash and rice husk ash. *Construction and Building Materials*, 21(6), 1356–1361.
- Chmelík, F., Trník, A., Štubňa, I., & Pešička, J. (2011). Creation of microcracks in porcelain during firing. *Journal of the European Ceramic Society*, 31(13), 2205–2209.
- Chouhan, R. K., Kujur, B., Amritphale, S. S., & CHANDRA, N. (2000). Effect of temperature of ashing of rice husk on the compressive strength of lime-rice husk silica mortar. *Silicates industriels*, (5-6), 67-71.
- Constâncio, C., Franco, L., Russo, A., Anjinho, C., Pires, J., Vaz, M. F., & Carvalho, A. P. (2010). Studies on polymeric conservation treatments of ceramic tiles with Paraloid B-72 and two alkoxysilanes. *Journal of Applied Polymer Science*, 116(5), 2833-2839.
- Cordeiro, G. C., Toledo Filho, R. D., & Fairbairn, E. D. M. R. (2009). Use of ultrafine rice husk ash with high-carbon content as pozzolan in high performance concrete. *Materials and structures*, 42(7), 983-992.
- Cordeiro, G. C., Toledo Filho, R. D., Tavares, L. M., Fairbairn, E. D. M. R., & Hempel, S. (2011). Influence of particle size and specific surface area on the pozzolanic activity of residual rice husk ash. *Cement and Concrete Composites*, 33(5), 529–534.
- da Silva, L. H., Feitosa, S. A., Valera, M. C., de Araujo, M. A., & Tango, R. N. (2012). Effect of the addition of silanated silica on the mechanical properties of microwave heat-cured acrylic resin. *Gerodontology*, 29(2), e1019-e1023.
- Daguano, J. K., Suzuki, P. A., Strecker, K., Fernandes, M. H., & Santos, C. (2012). Evaluation of the micro-hardness and fracture toughness of amorphous and partially crystallized 3CaO· P₂O₅–SiO₂–MgO bioglasses. *Materials Science and Engineering: A*, 533, 26-32.
- Dana, K., Das, S., & Das, S. K. (2004). Effect of substitution of fly ash for quartz in triaxial kaolin–quartz–feldspar system. *Journal of the European Ceramic Society*, 24(10), 3169-3175.
- Dana, K., Dey, J., & Das, S. K. (2005). Synergistic effect of fly ash and blast furnace slag on the mechanical strength of traditional porcelain tiles. *Ceramics international*, 31(1), 147-152.
- Das, K.S. & Dana, K. (2003) Differences in densification behaviour of K- and Na-Feldspar-containing porcelain bodies. *Thermochimica Acta* 406, pp 199-206.
- De Noni, A., Hotza, D., Soler, V. C., & Vilches, E. S. (2009). Effect of quartz particle size on the mechanical behaviour of porcelain tile subjected to different cooling rates. *Journal of the European Ceramic Society*, 29(6), 1039-1046.

- De Noni, A., Hotza, D., Soler, V. C., & Vilches, E. S. (2010). Influence of composition on mechanical behaviour of porcelain tile. Part I: Microstructural characterization and developed phases after firing. *Materials Science and Engineering: A*, 527(7), 1730-1735.
- de'Gennaro, R., Cappelletti, P., Cerri, G., de'Gennaro, M., Dondi, M., Guarini, G., ... & Naimo, D. (2003). Influence of zeolites on the sintering and technological properties of porcelain stoneware tiles. *Journal of the European Ceramic Society*, 23(13), 2237-2245.
- Derevyagina, A. A., Derevyagin, G. F., & Gaidash, B. I. (1980). Using kyanite—Sillimanite concentrate for making high-tension porcelain. *Glass and Ceramics*, 37(5), 252-255.
- Deshmukh, P., Bhatt, J., Peshwe, D., & Pathak, S. (2012). Determination of Silica Activity Index and XRD, SEM and EDS Studies of Amorphous SiO₂ Extracted from Rice Husk Ash. *Transactions of the Indian Institute of Metals*, 65(1), 63-70.
- Devaraj, A. R., Cheeseman, C. R., Boccaccini, A. R., & Deegan, D. (2010). Glass-Ceramic Tiles Prepared by Pressing and Sintering DC Plasma-Vitrified Air Pollution Control Residues. *International Journal of Applied Ceramic Technology*, 7(6), 925-934.
- Duku, M. H., Gu, S., & Hagan, E. B. (2011). Biochar production potential in Ghana—A review. *Renewable and Sustainable Energy Reviews*, 15(8), 3539-3551.
- Ece, O. I. and Nakagawa, Z. (2002) Bending Strength of Porcelains *Ceramics International* 28, pp 131-140.
- Eldagal, A., & Elmukhtar, O. (2008). *Study on the behaviour of high strength palm oil fuel ash (POFA) concrete* (Doctoral dissertation, Universiti Teknologi Malaysia, Faculty of Civil Engineering).
- El-Dakroury, a., & Gasser, M. S. (2008). Rice husk ash (RHA) as cement admixture for immobilization of liquid radioactive waste at different temperatures. *Journal of Nuclear Materials*, 381(3), 271–277.
- El-Maghraby, H. F., El-Omla, M. M., Bondioli, F., & Naga, S. M. (2011). Granite as flux in stoneware tile manufacturing. *Journal of the European Ceramic Society*, 31(12), 2057-2063.
- El-mahllawy, M. S., & Osman, T. A. (2010). Influence of Oil Well Drilling Waste on the Engineering Characteristics of Clay Bricks, 6(7), 48–54.
- Engelthaler, A. Z. and Engena, M. Y (January, 1972) Ceramic raw materials in Uganda, preliminary report *African Ceramics Company Ltd*, Kampala, Uganda.
- Esposito, L., Salem, A., Tucci, A., Gualtieri, A., & Jazayeri (2005). The use of nepheline-syenite in a body mix for porcelain stoneware tiles *Ceramics International* 31, pp 233-240.

- Fadzil, A. M., Azmi, M. M., Hisyam, A. B., & Azizi, M. K. (2008). Engineering Properties of Ternary Blended Cement Containing Rice Husk Ash and Fly Ash as Partial Cement Replacement Materials. *A* (10), 125-134.
- Farzadnia, N., Abang Ali, A. A., & Demirboga, R. (2011). Incorporation of mineral admixtures in sustainable high performance concrete. *International Journal of Sustainable Construction Engineering and Technology*, 2(1).
- Ferreira-Leitao, V., Gottschalk, L. M. F., Ferrara, M. A., Nepomuceno, A. L., Molinari, H. B. C., & Bon, E. P. (2010). Biomass residues in Brazil: availability and potential uses. *Waste and Biomass Valorization*, 1(1), 65-76.
- Foo, K. Y., & Hameed, B. H. (2009). Utilization of rice husk ash as novel adsorbent : A judicious recycling of the colloidal agricultural waste. *Advances in Colloid and Interface Science*, 152(1-2), 39–47.
- Frías, M., Vigil, R., García, R., Rodríguez, O., Goñi, S., & Vegas, I. (2012). Evolution of mineralogical phases produced during the pozzolanic reaction of different metakaolinite by-products: Influence of the activation process. *Applied Clay Science*, 56, 48-52.
- Furlani, E., Brückner, S., Minichelli, D., & Maschio, S. (2008). Synthesis and characterization of ceramics from coal fly ash and incinerated paper mill sludge. *Ceramics International*, 34(8), 2137-2142.
- Gadde, B., Bonnet, S., Menke, C., & Garivait, S. (2009). Air pollutant emissions from rice straw open field burning in India, Thailand and the Philippines. *Environmental Pollution*, 157(5), 1554-1558.
- Galos, K. (2011). Composition and ceramic properties of ball clays for porcelain stoneware tiles manufacture in Poland. *Applied clay science*, 51(1), 74-85.
- García Ten, J., Orts, M. J., Saburit, A., & Silva, G. (2010). Thermal conductivity of traditional ceramics. Part I: Influence of bulk density and firing temperature. *Ceramics International*, 36(6), 1951-1959.
- Garcia-Ten, J., Saburit, A., Bernardo, E., & Colombo, P. (2012). Development of lightweight porcelain stoneware tiles using foaming agents. *Journal of the European Ceramic Society*, 32(4), 745-752.
- Gastaldini, a. L. G., Isaia, G. C., Gomes, N. S., & Sperb, J. E. K. (2007). Chloride penetration and carbonation in concrete with rice husk ash and chemical activators. *Cement and Concrete Composites*, 29(3), 176–180.
- Gastaldini, a. L. G., Isaia, G. C., Hoppe, T. F., Missau, F., & Saciloto, A. P. (2009). Influence of the use of rice husk ash on the electrical resistivity of concrete: A technical and economic feasibility study. *Construction and Building Materials*, 23(11), 3411–3419.

- Ghasemi, Z., Younesi, H., & Kazemian, H. (2011). Synthesis of nanozeolite sodalite from rice husk ash without organic additives. *The Canadian Journal of Chemical Engineering*, 89(3), 601-608.
- Ghosh, T. B., Nandi, K. C., Acharya, H. N., & Mukherjee, D. (1991). XPS studies of magnesium silicide obtained from rice husk. *Materials Letters*, 11(1), 6-9.
- Givi, A. N., Rashid, S. A., Aziz, F. N. A., & Salleh, M. A. M. (2010). Assessment of the effects of rice husk ash particle size on strength, water permeability and workability of binary blended concrete. *Construction and Building Materials*, 24(11), 2145-2150.
- Gopal, J. (2001) The Development of Malaysia's Palm Oil Refining Industry: Obstacles, Policy and Performance. Ph.D. Thesis of the University of London and Diploma of Imperial College, England.
- Grimshaw, R. W., & Searle, A. B. (1971). *The chemistry and physics of clays and allied ceramic materials*. Wiley-Interscience.
- Guo, X., Wang, S., Wang, Q., Guo, Z., & Luo, Z. (2011). Properties of bio-oil from fast pyrolysis of rice husk. *Chinese Journal of Chemical Engineering*, 19(1), 116-121.
- Habeeb, G. A., & Fayyadh, M. M. (2009). Rice Husk Ash Concrete : the Effect of RHA Average Particle Size on Mechanical Properties and Drying Shrinkage, 3(3), 1616–1622.
- Hand, R.J., Stevens, S.J. & Sharp, J.H. (1998). “Characterisation of fired silicas”, *Thermochimica Acta*, 318, 115-123.
- Handreck, K. A., & Jones, L. H. P. (1968). Studies of silica in the oat plant. *Plant and Soil*, 29(3), 449-459.
- Hanna, S. B., Farag, L. M., & Mansour, N. A. (1984). Pyrolysis and combustion of treated and untreated rice hulls. *Thermochimica Acta*, 81, 77-86.
- Harish, K. V., Rangaraju, P. R., & Vempati, R. K. (2010). Fundamental investigations into performance of carbon-neutral rice husk ash as supplementary cementitious material. Transportation Research Record: Journal of the Transportation Research Board, 2164(1), 26-35.
- Haslinawati, M. M., Matori, K. A., Wahab, Z. A., Sidek, H. A. A., & Zainal, A. T. (2009). Effect of temperature on ceramic from rice husk ash. *International Journal of Basic & Applied Sciences*, 9(9), 111-117.
- Hassan, J. U., Noh, M. Z., & Ahmad, Z. A. (2014). Effects of Palm Oil Fuel Ash Composition on the Properties and Morphology of Porcelain-palm Oil Fuel Ash Composite. *Jurnal Teknologi*, 70(5).
- He, D., Wang, P., Liu, P., & Liu, X. (2012). Interface Bond Mechanism of EVA-Modified Mortar and Porcelain Tile. *Journal of Materials in Civil Engineering*, 25(6), 726-730.

- Heim, W. F., & McDowell, H. L. (1982). U.S. Patent No. 4,342,632. Washington, DC: U.S. Patent and Trademark Office.
- Hojamberdiev, M., Eminov, A., & Xu, Y. (2011). Utilization of muscovite granite waste in the manufacture of ceramic tiles. *Ceramics International*, 37(3), 871-876.
- Höland, W., Rheinberger, V., Apel, E., van't Hoen, C., Höland, M., Dommann, A., ... & Graf-Hausner, U. (2006). Clinical applications of glass-ceramics in dentistry. *Journal of Materials Science: Materials in Medicine*, 17(11), 1037-1042.
- Houston, D. F. (1972). Rice Chemistry and Technology, American Association of Cereal Chemist. Inc, Minnesota.
- Hunt, L. P., Dismukes, J. P., Amick, J. A., Schei, A., & Larsen, K. (1984). Rice hulls as a raw material for producing silicon. *Journal of the Electrochemical Society*, 131(7), 1683-1686.
- Hussain, R. R., & Ishida, T. (2010). Development of numerical model for FEM computation of oxygen transport through porous media coupled with micro-cell corrosion model of steel in concrete structures. *Computers & structures*, 88(9), 639-647.
- Hussain, R. R., & Ishida, T. (2011). Investigation of volumetric effect of coarse aggregate on corroding steel reinforcement at the interfacial transition zone of concrete. *KSCE Journal of Civil Engineering*, 15(1), 153-160.
- Iqbal, Y and Lee, W.E (2000) "Microstructural evolution in Triaxial porcelain" J. Am. Ceram. Soc. 83 [12] pp 3121-27.
- Iqbal, Y., & Lee, W. E. (1999). Fired porcelain microstructures revisited. *Journal of the American Ceramic Society*, 82(12), 3584-3590.
- Iqbal, Y., & Lee, W. E. (2000). Microstructural evolution in triaxial porcelain. *Journal of the American Ceramic Society*, 83(12), 3121-3127.
- Isaia, G. ., Gastaldini, a. L. ., & Moraes, R. (2003). Physical and pozzolanic action of mineral additions on the mechanical strength of high-performance concrete. *Cement and Concrete Composites*, 25(1), 69-76. Ismail, S., & Waliuddints, A. M. (1996). Effect of rice husk ash on high strength concrete, 10(I), 521-526.
- Ishak, Z. M., Bakar, A. A., Ishiaku, U. S., Hashim, A. S., & Azahari, B. (1997). An investigation of the potential of rice husk ash as a filler for epoxidized natural rubber—II. Fatigue behaviour. *European polymer journal*, 33(1), 73-79.
- Islam, R. A., Chan, Y.C, and Islam M. F. (2004) Structure-property relationship in high-tension ceramic insulator fired at high temperature *Materials Science and Engineering B106*, pp 132-140.
- Ismail, M. E., Budiea, A., Hussin, M. W., & Muthusamy, K. (2010). Effect of POFA fineness towards durability of POFA cement based high strength concrete. *The Indian Concrete Journal*.

- James, J., & Subba Rao, M. (1986). Reactivity of rice husk ash. *Cement and concrete research*, 16(3), 296-302.
- James, K. A. C., Bray, J. J., Morgan, I. G., & Austin, L. (1970). The effect of colchicine on the transport of axonal protein in the chicken. *Biochem. J*, 117, 767-771.
- Jamo, H. U., Noh, M. Z., & Ahmad, Z. A. (2013). Structural analysis and surface morphology of a treated palm oil fuel ash.
- Jamo, H. U., Noh, M. Z., & Ahmad, Z. A. (2014). Influence of Temperature on the Substitution of Quartz by Rice Husk Ash (RHA) in Porcelain Composition. *Applied Mechanics and Materials*, 465, 1297-1303.
- Jaturapitakkul, C., Kiattikomol, K., Tangchirapat, W., & Saeting, T. (2007). Evaluation of the sulfate resistance of concrete containing palm oil fuel ash. *Construction and Building Materials*, 21(7), 1399-1405.
- Johari, M., Zeyad, A. M., Muhamad Bunnori, N., & Ariffin, K. S. (2012). Engineering and transport properties of high-strength green concrete containing high volume of ultrafine palm oil fuel ash. *Construction and Building Materials*, 30, 281-288.
- Kalapathy, U., Proctor, A., & Shultz, J. (2000). A simple method for production of pure silica from rice hull ash. *Bioresource Technology*, 73(3), 257-262.
- Kamseu, E., Leonelli, C., Boccaccini, D. N., Veronesi, P., Miselli, P., Pellacani, G., & Melo, U. C. (2007). Characterisation of porcelain compositions using two china clays from Cameroon. *Ceramics international*, 33(5), 851-857.
- Kapur, P. C. (1985). Production of reactive bio-silica from the combustion of rice husk in a tube-in-basket (TiB) burner. *Powder technology*, 44(1), 63-67.
- Karamanov, A., Karamanova, E., Ferrari, A. M., Ferrante, F., & Pelino, M. (2006). The effect of fired scrap addition on the sintering behaviour of hard porcelain. *Ceramics international*, 32(7), 727-732.
- Karim, M. R., Zain, M. E. M., Jamil, M., Lai, F. C., & Islam, M. N. (2011). Strength development of mortar and concrete containing fly ash: A review. *International Journal of Physical . Sciences*, 6(17), 4137-4153.
- Kaya, G., Karasu, B., & Cakir, A. (2011). Characterisation of diopside-based glass-ceramic porcelain tile glazes containing borax solid wastes. *Journal of Ceramic Processing Research*, 12(2), 135-139.
- Ke, S., Cheng, X., Wang, Y., Wang, Q., & Wang, H. (2012). Dolomite, wollastonite and calcite as different CaO sources in anorthite-based porcelain. *Ceramics International*.
- Kingery, W. D. (1986). The development of European porcelain. In *High-Technology Ceramics: Past, Present, and Future-The Nature of Innovation and Change in Ceramic Technology* (Vol. 3, pp. 153-180). The American Ceramic Society, Inc..
- Kitouni, S., & Harabi, A. (2011). Sintering and mechanical properties of porcelains prepared from algerian raw materials. *Cerâmica*, 57(344), 453-460.

- Klankaw, P., Chawengkijwanich, C., Grisdanurak, N., & Chiarakorn, S. (2012). The hybrid photocatalyst of $\text{TiO}_2\text{-SiO}_2$ thin film prepared from rice husk silica. *Superlattices and Microstructures*, 51(3), 343-352.
- Kobayashi, K., Komine, F., Blatz, M. B., Saito, A., Koizumi, H., & Matsumura, H. (2009). Influence of priming agents on the short-term bond strength of an indirect composite veneering material to zirconium dioxide ceramic. *Quintessence international (Berlin, Germany: 1985)*, 40(7), 545.
- Kobayashi, Y. (1987). Strength and weibull distribution of alumina strengthened whiteware bodies. *Ceramic Society Japan*, 95(9), 887.
- Kolloor, S. S. R., Kashani, J., & Kadir, M. A. (2011, January). Simulation of Brittle Damage for Fracture Process of Endodontically Treated Tooth. In *5th Kuala Lumpur International Conference on Biomedical Engineering 2011* (pp. 210-214). Springer Berlin Heidelberg.
- Kordani, N., Asadi, A., & Jabbari, A. (2012). Optimization of fracture behavior of alumina/silicon carbide nano ceramic. *Neural Computing and Applications*, 1-7.
- Kroehong, W., Sinsiri, T., Jaturapitakkul, C., & Chindaprasirt, P. (2011). Effect of palm oil fuel ash fineness on the microstructure of blended cement paste. *Construction and Building Materials*, 25(11), 4095-4104.
- Kurama, S., & Kurama, H. (2008). The reaction kinetics of rice husk based cordierite ceramics. *Ceramics International*, 34(2), 269-272.
- LaSalvia, J. C., Campbell, J., Swab, J. J., & McCauley, J. W. (2010). Beyond hardness: ceramics and ceramic-based composites for protection. *JOM*, 62(1), 16-23.
- Lee, D. J., Jang, J. J., Park, H. S., Kim, Y. C., Lim, K. H., Park, S. B., & Hong, S. H. (2012). Fabrication of biomorphic SiC composites using wood preforms with different structures. *Ceramics International*, 38(4), 3089-3095.
- Lee, W. E. (1994). *Ceramic microstructures: property control by processing*. Springer.
- Lee, W. E., & Iqbal, Y. (2001). Influence of mixing on mullite formation in porcelain. *Journal of the European Ceramic Society*, 21(14), 2583-2586.
- Lee, W. E., & Iqbal, Y. (2001). Influence of mixing on mullite formation in porcelain. *Journal of the European Ceramic Society*, 21(14), 2583-2586.
- Lee, W. E., Souza, G. P., McConville, C. J., Tarvornpanich, T., & Iqbal, Y. (2008). Mullite formation in clays and clay-derived vitreous ceramics. *Journal of the European Ceramic Society*, 28(2), 465-471.
- Leonelli, C., Bondioli, F., Veronesi, P., Romagnoli, M., Manfredini, T., Pellacani, G. C., & Cannillo, V. (2001). Enhancing the mechanical properties of porcelain stoneware tiles: a microstructural approach. *Journal of the European Ceramic Society*, 21(6), 785-793.

- Leonelli, C., Bondioli, F., Veronesi, P., Romagnoli, M., Manfredini, T., Pellacani, G. C., & Cannillo, V. (2001). Enhancing the mechanical properties of porcelain stoneware tiles: a microstructural approach. *Journal of the European Ceramic Society*, 21(6), 785-793.
- Li, Y., Ding, X., Guo, Y., Rong, C., Wang, L., Qu, Y., & Wang, Z. (2011). A new method of comprehensive utilization of rice husk. *Journal of hazardous materials*, 186(2), 2151-2156.
- Li, Y., Zhao, C., Ren, Q., Duan, L., Chen, H., & Chen, X. (2009). Effect of rice husk ash addition on CO₂ capture behavior of calcium-based sorbent during calcium looping cycle. *Fuel Processing Technology*, 90(6), 825-834.
- Li, Z., Tang, S., Deng, X., Wang, R., & Song, Z. (2010). Contrasting effects of elevated CO₂ on Cu and Cd uptake by different rice varieties grown on contaminated soils with two levels of metals: Implication for phytoextraction and food safety. *Journal of hazardous materials*, 177(1), 352-361.
- Liou, T. H. (2004). Preparation and characterization of nano-structured silica from rice husk. *Materials Science and Engineering: A*, 364(1), 313-323.
- Liu, J., Zehnder, A. J., & Yang, H. (2009). Global consumptive water use for crop production: The importance of green water and virtual water. *Water Resources Research*, 45(5).
- Lopez, S. Y. R., Yobanny, S., Serrato Rodriguez, J., & Sugita Sueyoshi, S. (2011). Determination of the activation energy for densification of porcelain stoneware. *Journal of Ceramic Processing Research*, 12(3), 228-232.
- Lundin, S. T. (1964). Microstructure of porcelain. *Microstructure of Ceramic Materials*. NBS Misc. Publ, 257, 93-106.
- Luz, A. P., & Ribeiro, S. (2007). Use of glass waste as a raw material in porcelain stoneware tile mixtures. *Ceramics international*, 33(5), 761-765.
- Ma, X., Zhou, B., Gao, W., Qu, Y., Wang, L., Wang, Z., & Zhu, Y. (2012). A recyclable method for production of pure silica from rice hull ash. *Powder*
- Maity, S., & Sarkar, B. K. (1996). Development of High-Strength Whiteware Bodies, 2219(96).
- Maity, S., & Sarkar, B. K. (1996). Development of high-strength whiteware bodies. *Journal of the European Ceramic Society*, 16(10), 1083-1088.
- Maity, S., & Sarkar, B. K. (1996). Development of high-strength whiteware bodies. *Journal of the European Ceramic Society*, 16(10), 1083-1088.
- Maity, S., & Sarkar, B. K. (1996). Development of high-strength whiteware bodies. *Journal of the European Ceramic Society*, 16(10), 1083-1088.
- Malaysian Palm Oil Board (MPOB). Economic and statistic; 2013 http://econ.mpo.gov.my/economy/Overview_2009.pdf [accessed 12.05. 2012].

- Mane, V. S., Deo Mall, I., & Chandra Srivastava, V. (2007). Kinetic and equilibrium isotherm studies for the adsorptive removal of Brilliant Green dye from aqueous solution by rice husk ash. *Journal of Environmental Management*, 84(4), 390-400.
- Manfredini, T., Pellacani, G. C., Romagnoli, M., & Pennisi, L. (1995). Porcelainized stoneware tile. *American Ceramic Society Bulletin*, 74(5), 76-79
- Mansaray, K. G., & Ghaly, A. E. (1997). Physical and thermochemical properties of rice husk. *Energy Sources*, 19(9), 989-1004.
- Martin, J. I. (1938). *The desilification of rice husk and a study of the products obtained*. Louisiana State University, USA: Master Thesis.
- Martínez, J. D., Pineda, T., López, J. P., & Betancur, M. (2011). Assessment of the rice husk lean-combustion in a bubbling fluidized bed for the production of amorphous silica-rich ash. *Energy*, 36(6), 3846-3854.
- Martín-Márquez, J., De la Torre, A. G., Aranda, M. A., Rincón, J. M., & Romero, M. (2009). Evolution with temperature of crystalline and amorphous phases in porcelain stoneware. *Journal of the American Ceramic Society*, 92(1), 229-234.
- Martín-Márquez, J., Rincón, J. M., & Romero, M. (2008). Effect of firing temperature on sintering of porcelain stoneware tiles. *Ceramics International*, 34(8), 1867-1873.
- Martín-Márquez, J., Rincón, J. M., & Romero, M. (2010). Mullite development on firing in porcelain stoneware bodies. *Journal of the European Ceramic Society*, 30(7), 1599-1607.
- Martín-Márquez, J., Rincón, J. M., & Romero, M. (2010a). Effect of microstructure on mechanical properties of porcelain stoneware. *Journal of the European Ceramic Society*, 30(15), 3063-3069.
- Martín-Márquez, J., Rincón, J. M., & Romero, M. (2010b). Mullite development on firing in porcelain stoneware bodies. *Journal of the European Ceramic Society*, 30(7), 1599-1607.
- Matteucci, F., Dondi, M., & Guarini, G. (2002). Effect of soda-lime glass on sintering and technological properties of porcelain stoneware tiles. *Ceramics International*, 28(8), 873-880.
- Mehta, P. K., & Pitt, N. (1976). Energy and industrial materials from crop residues. *Resource Recovery and Conservation*, 2(1), 23-38.
- Mondragon, R., Jarque, J. C., Julia, J. E., Hernandez, L., & Barba, A. (2012). Effect of slurry properties and operational conditions on the structure and properties of porcelain tile granules dried in an acoustic levitator. *Journal of the European Ceramic Society*, 32(1), 59-70.
- Montoya, N., Serrano, F. J., Reventós, M. M., Amigo, J. M., & Alarcón, J. (2010). Effect of TiO_2 on the mullite formation and mechanical properties of alumina porcelain. *Journal of the European Ceramic Society*, 30(4), 839-846.

- Moradkhani, A. R., Baharvandi, H. R., Vafaeseefat, A., & Tajdari, M. (2012). Microstructure and Mechanical Properties of Al₂O₃-SiC Nanocomposites with 0.05% MgO and Different SiC Volume Fraction. *International Journal of Advanced Design and Manufacturing Technology*, 5(3), 99-105.
- Mukhopadhyay, T. K., Das, M., Ghosh, S., Chakrabarti, S., & Ghatak, S. (2003). Microstructure and thermo mechanical properties of a talc doped stoneware composition containing illitic clay. *Ceramics international*, 29(5), 587-597.
- Mukhopadhyay, T. K., Ghosh, S., Ghatak, S., & Maiti, H. S. (2006). Effect of pyrophyllite on vitrification and on physical properties of triaxial porcelain. *Ceramics international*, 32(8), 871-876.
- Mukhopadhyay, T. K., Ghosh, S., Ghatak, S., & Maiti, H. S. (2006). Effect of pyrophyllite on vitrification and on physical properties of triaxial porcelain. *Ceramics international*, 32(8), 871-876.
- Naga, S. M., Bondioli, F., Wahsh, M. M. S., & El-Omla, M. (2012). Utilization of granodiorite in the production of porcelain stoneware tiles. *Ceramics International*, 38(8), 6267-6272.
- Naivinit, W., Le Page, C., Trébuil, G., & Gajaseni, N. (2010). Participatory agent-based modeling and simulation of rice production and labor migrations in Northeast Thailand. *Environmental Modelling & Software*, 25(11), 1345-1358.
- Naskar, M. K., & Chatterjee, M. (2004). A novel process for the synthesis of cordierite (Mg₂Al₄Si₅O₁₈) powders from rice husk ash and other sources of silica and their comparative study. *Journal of the European Ceramic Society*, 24(13), 3499-3508.
- Natarajan, E., Öhman, M., Gabra, M., Nordin, A., Liliedahl, T., & Rao, A. N. (1998). Experimental determination of bed agglomeration tendencies of some common agricultural residues in fluidized bed combustion and gasification. *Biomass and Bioenergy*, 15(2), 163-169.
- Nayak, J. P., Kumar, S., & Bera, J. (2010). Sol-gel synthesis of bioglass-ceramics using rice husk ash as a source for silica and its characterization. *Journal of Non-Crystalline Solids*, 356(28), 1447-1451.
- Neklyudova, T. L., & Maslennikova, G. N. (2011). Structural particulars of porcelain articles manufactured by slip casting. *Glass and Ceramics*, 68(1), 52-55.
- Ngo, S. P. (2006). Production of amorphous silica from rice husk in fluidised bed system (Doctoral dissertation, Universiti Teknologi Malaysia, Faculty of Chemical Engineering and Natural Resources Engineering).
- Norton, F.H. (1970) *Fine Ceramics, Technology and Applications*. McGraw-Hill Book Co. New York.

- Okoronkwo, E. A., Imoisili, P. E., & Olusunle, S. O. O. (2013). Extraction and characterization of Amorphous Silica from Corn Cob Ash by Sol-Gel Method. *Chemistry and Materials Research*, 3(4), 68-72.
- Olgun, A., Erdogan, Y., Ayhan, Y., & Zeybek, B. (2005). Development of ceramic tiles from coal fly ash and tincal ore waste. *Ceramics International*, 31(1), 153-158.
- Olupot, P. W. (2006). Assessment of ceramic raw materials in Uganda for electrical porcelain (Doctoral dissertation, KTH).
- Pelaez-Vargas, A., Dussan, J. A., Restrepo-Tamayo, L. F., Paucar, C., Ferreira, J. A., & Monteiro, F. J. (2011). The effect of slurry preparation methods on biaxial flexural strength of dental porcelain. *The Journal of prosthetic dentistry*, 105(5), 308-314.
- Pérez, J. M., Rincón, J. M., & Romero, M. (2012). Effect of moulding pressure on microstructure and technological properties of porcelain stoneware. *Ceramics International*, 38(1), 317-325.
- Pinheiro, B. C. A., & Holanda, J. N. F. (2013). Reuse of solid petroleum waste in the manufacture of porcelain stoneware tile. *Journal of environmental management*, 118, 205-210.
- Porion, P., Busignies, V., Mazel, V., Leclerc, B., Evesque, P., & Tchoreloff, P. (2010). Anisotropic Porous Structure of Pharmaceutical Compacts Evaluated by PGSTE-NMR in Relation to Mechanical Property Anisotropy. *Pharmaceutical research*, 27(10), 2221-2233.
- Prasad, C. S., Maiti, K. N., & Venugopal, R. (2001). Effect of rice husk ash in whiteware compositions. *Ceramics International*, 27(6), 629-635.
- Prasad, C. S., Maiti, K. N., & Venugopal, R. (2003). Effect of substitution of quartz by rice husk ash and silica fume on the properties of whiteware compositions. *Ceramics international*, 29(8), 907-914.
- Prasad, C.S, Maiti, K.N. and Venugopal R. (2002) Effect of silica fume addition on the properties of whiteware compositions *Ceramics International* 28 pp 9-15
- Prasad, R., & Pandey, M. (2012). Rice husk ash as a renewable source for the production of value added silica gel and its application: an overview. *Bulletin of Chemical Reaction Engineering & Catalysis*, 7(1), 1-25.
- Prasad, S. D., & Krishna, R. A. (2011). Production and mechanical properties of A356. 2/RHA composites. *International Journal of Advanced Science and Technology*, 33, 51-58.
- Prasara-A, J. (2009). *Comparative Life Cycle Assessment of Rice Husk Utilization in Thailand* (Doctoral dissertation, RMIT University).
- Prasetyoko, D., Ramli, Z., Endud, S., & Hamdan, H. (2006a). Conversion of rice husk ash to zeolite beta, 26, 1173–1179.

- Rahaman, N. 2003. *Ceramic Processing and Sintering*, M. Dekker.
- Raimondo, M., Dondi, M., Zanelli, C., Guarini, G., Gozzi, A., Marani, F., & Fossa, L. (2010). Processing and properties of large-sized ceramic slabs. *Boletín de la Sociedad Española de Cerámica y Vidrio*, 49(4), 289-295.
- Rambaldi, E., Carty, W. M., Tucci, A., & Esposito, L. (2007). Using waste glass as a partial flux substitution and pyroplastic deformation of a porcelain stoneware tile body. *Ceramics international*, 33(5), 727-733.
- Rambaldi, E., Tucci, A., Esposito, L., Naldi, D., & Timellini, G. (2010). Nano-oxides to improve the surface properties of ceramic tiles. *Boletín de la Sociedad Española de Cerámica y Vidrio*, 49(4), 253-258.
- Ramesh, S., Tolouei, R., Hamdi, M., Purbolaksono, J., Y Tan, C., Amiriyan, M., & D Teng, W. (2011). Sintering Behavior of Nanocrystalline Hydroxyapatite Produced by Wet Chemical Method. *Current Nanoscience*, 7(6), 845-849.
- Randal, M. G. 1991. *Engineered Materials Handbook: Ceramics and Glasses*, Ohio.
- Rangaraju, P., & Harish, K. V. Optimization of Use of Rice Husk Ash for use as SCM in Cementitious Mortars.
- Rincón, J. Ma.,(1992). Principles of nucleation and controlled crystallization of glasses, *Polym. Plast. Technol. Eng.*, 31, 309-357.
- Rodríguez de Sensale, G. (2006). Strength development of concrete with rice-husk ash. *Cement and Concrete Composites*, 28(2), 158-160.
- Romero, M., Martín-Márquez, J., & Rincón, J. M. (2006). Kinetic of mullite formation from a porcelain stoneware body for tiles production. *Journal of the European Ceramic Society*, 26(9), 1647-1652.
- Rosa, V., Yoshimura, H. N., Pinto, M. M., Fredericci, C., & Cesar, P. F. (2009). Effect of ion exchange on strength and slow crack growth of a dental porcelain. *dental materials*, 25(6), 736-743.
- Rukzon, S., Chindapasirt, P., & Mahachai, R. (2009). Effect of grinding on chemical and physical properties of rice husk ash. *International Journal of Minerals, Metallurgy and Materials*, 16(2), 242-247.
- Safiuddin, M., Abdus Salam, M., & Jumaat, M. Z. (2011). Utilization of palm oil fuel ash in concrete: a review. *Journal of Civil Engineering and Management*, 17(2), 234-247.
- Safiuddin, M., Jumaat, M. Z., Salam, M. A., Islam, M. S., & Hashim, R. (2010). Utilization of solid wastes in construction materials. *International Journal of Physical Sciences*, 5(13), 1952-1963.

- Saidur, R., Abdelaziz, E. A., Demirbas, A., Hossain, M. S., & Mekhilef, S. (2011). A review on biomass as a fuel for boilers. *Renewable and Sustainable Energy Reviews*, 15(5), 2262-2289.
- Salem, A., Jazayeri, S. H., Rastelli, E., & Timellini, G. (2010). Kinetic model for isothermal sintering of porcelain stoneware body in presence of nepheline syenite. *Thermochimica Acta*, 503, 1-7.
- Sanchez, E., Ibanez, M. J., García-Ten, J., Quereda, M. F., Hutchings, I. M., & Xu, Y. M. (2006). Porcelain tile microstructure: Implications for polished tile properties. *Journal of the European Ceramic Society*, 26(13), 2533-2540.
- Sanchez, E., Orts, M. J., Garcia-Ten, J., & Cantavella, V. (2001). Porcelain tile composition effect on phase formation and end products. *American Ceramic Society Bulletin*, 80(6), 43-49.
- Santos, T., Costa, L. C., Henrietier, L., Valente, M. A., Monteiro, J., & Sousa, J. (2012). Microwave processing of porcelain tableware using a multiple generator configuration. *Applied Thermal Engineering*.
- Sarangi, M., Bhattacharyya, S., & Behera, R. C. (2009). Effect of temperature on morphology and phase transformations of nano-crystalline silica obtained from rice husk. *Phase Transitions*, 82(5), 377-386.
- Saravanan, K., Yuvakkumar, R., Rajendran, V., & Paramasivam, P. (2012). Influence of sintering temperature and pH on the phase transformation, particle size and anti-reflective properties of RHA nano silica powders. *Phase Transitions*, 85(12), 1109-1124.
- Sata, V., Jaturapitakkul, C., & Kiattikomol, K. (2007). Influence of pozzolan from various by-product materials on mechanical properties of high-strength concrete. *Construction and Building Materials*, 21(7), 1589-1598.
- Sata, V., Jaturapitakkul, C., & Rattanashotinunt, C. (2010). Compressive strength and heat evolution of concretes containing palm oil fuel ash. *Journal of Materials in Civil Engineering*, 22(10), 1033-1038.
- Sata, V., Jaturapitakkul, C., & Rattanashotinunt, C. (2010). Compressive strength and heat evolution of concretes containing palm oil fuel ash. *Journal of Materials in Civil Engineering*, 22(10), 1033-1038.
- Sata, V., Tangpagasit, J., Jaturapitakkul, C., & Chindaprasirt, P. (2012). Effect of W/B ratios on pozzolanic reaction of biomass ashes in Portland cement matrix. *Cement and Concrete Composites*, 34(1), 94-100.
- Schey, J.A. (2000). *Introduction to Manufacturing Processes* 3rd ed. U.S.A.: McGraw Hill Higher Education pp476-489.
- Schroeder, E. J. (1978) Inexpensive high strength electrical porcelain Am. Ceram. Soc. Bull. 57, 526.

- Schuller, K.H. (1964) Reactions between mullite and glassy in porcelain, *Trans. J. Brit. Ceram. Soc.* 63 pp 103.
- Sharma, P., Kaur, R., Baskar, C., & Chung, W. J. (2010). Removal of methylene blue from aqueous waste using rice husk and rice husk ash. *Desalination*, 259(1), 249-257.
- Shibib, K. S., Qatta, H. I., & Hamza, M. S. (2012). Enhancement in thermal and mechanical properties of bricks. *Thermal Science*, (00), 43-43.
- Shu, Z., Garcia-Ten, J., Monfort, E., Amoros, J. L., Zhou, J., & Wang, Y. X. (2012). Cleaner duction of porcelain tile powders. Granule and green compact characterization. *Ceramics International*, 38(1), 517-526.
- Shui, A., Xi, X., Wang, Y., & Cheng, X. (2011). Effect of silicon carbide additive on microstructure and properties of porcelain ceramics. *Ceramics International*, 37(5), 1557-1562.
- Singer, F. Singer, S.S. (1971). *Industrial Ceramics*, Chapman and Hall, London
- Siqueira, E. J., Yoshida, I. V. P., Pardini, L. C., & Schiavon, M. A. (2009). Preparation and characterization of ceramic composites derived from rice husk ash and polysiloxane. *Ceramics International*, 35(1), 213-220.
- Snel, M. D., Snijkers, F., Luyten, J., & Kodentsov, A. (2007). Aqueous tape casting of reaction bonded aluminium oxide (RBAO). *Journal of the European Ceramic Society*, 27(1), 27-33.
- Sokolar, R., & Smetanova, L. (2010). Dry pressed ceramic tiles based on fly ash–clay body: influence of fly ash granulometry and pentasodium triphosphate addition. *Ceramics international*, 36(1), 215-221.
- Sokolar, R., & Vodova, L. (2011). The effect of fluidized fly ash on the properties of dry pressed ceramic tiles based on fly ash–clay body. *Ceramics International*, 37(7), 2879-2885.
- Sokolar, R., & Vodova, L. (2011). The effect of fluidized fly ash on the properties of dry pressed ceramic tiles based on fly ash–clay body. *Ceramics International*, 37(7), 2879-2885.
- Sonuparlak, M. Sarikaya, and I. A. Aksay, (1987).“Spinel Phase Formation during 980°C Exothermic Reaction in the Kaolinite-to-Mullite Reaction Series,” *J. Am. Ceram. Soc.*, 70 [III 83742 ., 70 [III 83742
- Sooksaen, P. (2011). Effect of alumina content on the properties of ceramic foams crystallized with nano-sized mullite crystals. In *Materials Science Forum* (Vol. 694, pp. 456-460).
- Soraru, G. D., & Tassone, P. (2004). Mechanical durability of a polymer concrete: a Vickers indentation study of the strength degradation process. *Construction and Building Materials*, 18(8), 561-566.

- Standard A.S.T.M. (2011). C773-88(2011) Standard Test Method for Compressive (Crushing) Strength of Fired Whitewares Materials , ASTM, West Conshohocken, PA.
- Standard, A. S. T. M. (2006). C373-88(2006). Standard test method for water absorption, bulk density, apparent density and the apparent specific gravity of fired whiteware products. *American Society for Testing Materials*, West Conshohocken, PA.
- Standard, A. S. T. M. (2008). C1161-02 (2008) . Standard test method for flexural strength of advanced ceramics at ambient temperature. West Conshohocken, PA.
- Standard, A.S.T.M.(2008).C1327. Standard test method for Vickers indentation hardness of advanced ceramics. *Materials* , ASTM, West Conshohocken, PA tion for Testing Materials; 1999.
- Stathis, G., Ekonomakou, A., Stournaras, C.J, and Ftikos, C. (2004) Effect of firing conditions, filler grain size and quartz content on bending strength and physical properties of sanitary ware porcelain *Journal of the European Ceramic Society* 24, pp 2357-2366.
- Stathis, G., Ekonomakou, A., Stournaras, C.J, and Ftikos, C. (2004) Effect of firing conditions, filler grain size and quartz content on bending strength and physical properties of sanitary ware porcelain *Journal of the European Ceramic Society* 24, pp 2357-2366.
- Sumran, M., & Kongkachuichay, P. (2013). Synthesis of Silica from Rice Husk by One-step Combustion, Fluidized Bed Combustion, and Alkaline Extraction. *KKU Engineering Journal*, 30(2), 165-172.
- Suvaci, E., & Tamsu, N. (2010). The role of viscosity on microstructure development and stain resistance in porcelain stoneware tiles. *Journal of the European Ceramic Society*, 30(15), 3071-3077.
- Tai, Weon-Pil. Kimura, K. and Jinnai K. (2002) “A new approach to anorthite porcelain bodies using non-plastic raw materials” *Journal of the European Ceramic Society* 22, pp 463-470.
- Tangchirapat, W., & Jaturapitakkul, C. (2010). Strength, drying shrinkage, and water permeability of concrete incorporating ground palm oil fuel ash. *Cement and Concrete Composites*, 32(10), 767-774.
- Tangchirapat, W., Jaturapitakkul, C., & Chindaprasirt, P. (2009). Use of palm oil fuel ash as a supplementary cementitious material for producing high-strength concrete. *Construction and Building Materials*, 23(7), 2641-2646.
- Tarvornpanich, T., Souza, G. P., & Lee, W. E. (2008). Microstructural Evolution in Clay-Based Ceramics II: Ternary and Quaternary Mixtures of Clay, Flux, and Quartz Filler. *Journal of the American Ceramic Society*, 91(7), 2272-2280.

- Tasić, Ž. D. (1993). Improving the microstructural and physical properties of alumina electrical porcelain with Cr₂O₃, MnO₂ and ZnO additives. *Journal of materials science*, 28(21), 5693-5701.
- Tay, J. H. (1990). Ash from oil-palm waste as a concrete material. *Journal of Materials in Civil Engineering*, 2(2), 94-105.
- Tay, J. H., & Show, K. Y. (1995). Use of ash derived from oil-palm waste incineration as a cement replacement material. *Resources, conservation and recycling*, 13(1), 27-36.
- Tenorio Cavalcante, P. M., Dondi, M., Ercolani, G., Guarini, G., Melandri, C., Raimondo, M., & Rocha e Almendra, E. (2004). The influence of microstructure on the performance of white porcelain stoneware. *Ceramics international*, 30(6), 953-963.
- Thompson, M., Fahrenholtz, W. G., & Hilmas, G. (2011). Effect of starting particle size and oxygen content on densification of ZrB₂. *Journal of the American Ceramic Society*, 94(2), 429-435.
- Thurnauer, H. (1954) *Dielectric Materials and Applications* (A.R.V. Hippel, Ed.)
- Tian, X., Günster, J., Melcher, J., Li, D., & Heinrich, J. G. (2009). Process parameters analysis of direct laser sintering and post treatment of porcelain components using Taguchi's method. *Journal of the European Ceramic Society*, 29(10), 1903-1915.
- Tolouei, R., Singh, R., Sopyan, I., Tan, C. Y., Amiriyan, M., & Teng, W. D. (2011). Dependence of the Fracture Toughness on the Sintering Time of Dense Hydroxyapatite Bioceramics. In *Materials Science Forum* (Vol. 694, pp. 391-395).
- Tomizaki, M. F., & Shinkai, S. (1995). Influence of the grain size of alumina in the glaze of fast-fired porcelain tiles. *Nippon seramikusu kyokai gakujutsu ronbunshi*, 103(4), 325-329.
- Tonnayopas D, Nilrat F, Putto K, Tantiwitayawanich J (2006). Effect of Oil Palm Fiber Fuel Ash on Compressive Strength of Hardened Concrete. In: Proceedings of the Fourth Thailand Materials Science and Technology Conference, Pathumthani, Thailand. pp.1-3.
- Tonnayopas, D., Kooptarnond, K., & Masae, M. (2009). Novel Ecological Tiles Made with Granite Fine Quarry Waste and Oil Palm Fiber Ash. *Thammasat Int. J. Sc. Tech*, 14(1).
- Torres, Y., Pavón, J. J., & Rodríguez, J. A. (2012). Processing and characterization of porous titanium for implants by using NaCl as space holder. *Journal of Materials Processing Technology*, 212(5), 1061-1069.
- Tucci, A., Esposito, L., Malmusi, L., & Rambaldi, E. (2007). New body mixes for porcelain stoneware tiles with improved mechanical characteristics. *Journal of the European Ceramic Society*, 27(2), 1875-1881.

- Tucci, A., Esposito, L., Rastelli, E., Palmonari, C., & Rambaldi, E. (2004). Use of soda-lime scrap-glass as a fluxing agent in a porcelain stoneware tile mix. *Journal of the European Ceramic Society*, 24(1), 83-92.
- Tucci, A., Esposito, L., Rastelli, E., Palmonari, C., & Rambaldi, E. (2004). Use of soda-lime scrap-glass as a fluxing agent in a porcelain stoneware tile mix. *Journal of the European Ceramic Society*, 24(1), 83-92.
- Tuck, C. O., Pérez, E., Horváth, I. T., Sheldon, R. A., & Poliakoff, M. (2012). Valorization of biomass: deriving more value from waste. *Science*, 337(6095), 695-699.
- Usman, J., Arifin, Z., & Zaky, M. (2012). The effects of Rice Husk Ash on Porcelain composition, 2012(Rafss).
- Van Tuan, N., Ye, G., Van Breugel, K., Fraaij, A. L., & Bui, D. D. (2011). The study of using rice husk ash to produce ultra high performance concrete. *Construction and Building Materials*, 25(4), 2030-2035.
- Vandeperre, L. J., Wang, J., & Clegg†, W. J. (2004). Effects of porosity on the measured fracture energy of brittle materials. *Philosophical Magazine*, 84(34), 3689-3704.
- Vargas-Gonzalez, L., Speyer, R. F., & Campbell, J. (2010). Flexural strength, fracture toughness, and hardness of silicon carbide and boron carbide armor ceramics. *International Journal of Applied Ceramic Technology*, 7(5), 643-651.
- Vásquez, V., Özcan, M., Nishioka, R., Souza, R., Mesquita, A., & Pavanelli, C. (2008). Mechanical and Thermal Cycling Effects on the Flexural Strength of Glass Ceramics Fused to Titanium, 27(1).
- Vempati, R. K. (2002). U.S. Patent No. 6,444,186. Washington, DC: U.S. Patent and Trademark Office.
- Vempati, Rajan K., et al. "Surface analyses of pyrolysed rice husk using scanning force microscopy." *Fuel* 74.11 (1995): 1722-1725.
- Vieira, C. M. F., & Monteiro, S. N. (2007). Evaluation of a Plastic Clay from the State of Rio de Janeiro as a Component of Porcelain Tile Body, 1-7.
- Vieira, C. M. F., Peçanha Jr, L. A., & Monteiro, S. N. (2006). Effect of kaolinitic clays from the State of Rio de Janeiro in the composition of whiteware floor tile bodies. *Cerâmica*, 52(322), 138-145.
- Vinh, P. P., van Tol, I. A., van Paassen, I. L., & Ye, G. (2012). Utilization of Rice husk ash in GeoTechnology. *GeoScience*.
- Wansom, S., Janjaturaphan, S., & Sinthupinyo, S. (2010). Characterizing pozzolanic activity of rice husk ash by impedance spectroscopy. *Cement and Concrete Research*, 40(12), 1714-1722. Xu, W., Lo, T. Y., & Memon, S. A. (2012).

- Microstructure and reactivity of rich husk ash. *Construction and Building Materials*, 29, 541–547.
- Warshaw, S. I., & Seider, R. (1967). Comparison of strength of triaxial porcelains containing alumina and silica. *Journal of the American Ceramic Society*, 50(7), 337-343.
- Wei, Q., Gao, W., & Sui, X. (2010). Synthesis of low-temperature, fast, single-firing body for porcelain stoneware tiles with coal gangue. *Waste Management & Research*, 28(10), 944-950.
- Wetzel, A., Zurbriggen, R., & Herwegh, M. (2010). Spatially resolved evolution of adhesion properties of large porcelain tiles. *Cement and Concrete Composites*, 32(5), 327-338.
- Whittenberger, R. T. (1945). Silicon absorption by rye and sunflower. *American Journal of Botany*, 539-549.
- Wongpa, J., Kiattikomol, K., Jaturapitakkul, C., & Chindaprasirt, P. (2010). Compressive strength, modulus of elasticity, and water permeability of inorganic polymer concrete. *Materials & Design*, 31(10), 4748-4754.
- Wu, C. Z., Yin, X. L., Yuan, Z. H., Zhou, Z. Q., & Zhuang, X. S. (2010). The development of bioenergy technology in China. *Energy*, 35(11), 4445-4450.
- Wu, J., Leung, P. L., Li, J. Z., Stokes, M. J., & Li, M. T. W. (2000). EDXRF studies on blue and white Chinese Jingdezhen porcelain samples from the Yuan, Ming and Qing dynasties, (March 1999), 239–244.
- Yalc, N., & Sevinc, V. (2001). Studies on silica obtained from rice husk, 27, 219–224.
- Yan, X., Akiyama, H., Yagi, K., & Akimoto, H. (2009). Global estimations of the inventory and mitigation potential of methane emissions from rice cultivation conducted using the 2006 Intergovernmental Panel on Climate Change Guidelines. *Global Biogeochemical Cycles*, 23(2).
- Youssef, M. M., & Ghazal, H. B. G. (2011). Characterization and Reuse of Kiln Rollers Waste in the Manufacture of Ceramic Floor Tiles. *Journal of American Science*, 7(5).
- Yuvakkumar, R., Elango, V., Rajendran, V., & Kannan, N. (2012). High-purity nano silica powder from rice husk using a simple chemical method. *Journal of Experimental Nanoscience*, (ahead-of-print), 1-10.
- Zain, M. F. M., Islam, M. N., Mahmud, F., & Jamil, M. (2011). Production of rice husk ash for use in concrete as a supplementary cementitious material. *Construction and Building Materials*, 25(2), 798–805.
- Zain, M. F. M., Islam, M. N., Mahmud, F., & Jamil, M. (2011). Production of rice husk ash for use in concrete as a supplementary cementitious material. *Construction and building materials*, 25(2), 798-805.

- Zanelli, C., Raimondo, M., Guarini, G., & Dondi, M. (2011). The vitreous phase of porcelain stoneware: Composition, evolution during sintering and physical properties. *Journal of Non-Crystalline Solids*, 357(16), 3251-3260.
- Zarone, F., Russo, S., & Sorrentino, R. (2011). From porcelain-fused-to-metal to zirconia: clinical and experimental considerations. *Dental materials*, 27(1), 83-96.
- Zhang, H., Guo, T. W., Song, Z. X., Wang, X. J., & Xu, K. W. (2006). The effect of ZrSiN diffusion barrier on the bonding strength of titanium porcelain, 1–4.
- Zhang, H., Zhao, X., Ding, X., Lei, H., Chen, X., An, D., & Wang, Z. (2010). A study on the consecutive preparation of d-xylose and pure superfine silica from rice husk. *Bioresource technology*, 101(4), 1263-1267.
- Zou, C., Zhang, C., Li, B., Wang, S., & Cao, F. (2012). Microstructure and properties of porous silicon nitride ceramics prepared by gel-casting and gas pressure sintering. *Materials & Design*.
- Zuda, L., Drchalová, J., Rovnaník, P., Bayer, P., Keršner, Z., & Černý, R. (2010). Alkali-activated aluminosilicate composite with heat-resistant lightweight aggregates exposed to high temperatures: Mechanical and water transport properties. *Cement and Concrete Composites*, 32(2), 157-163.790. (n.d.)
- Zuur, K. (2004) *Sustainability through Environmental Technology: A Case Study on Malaysia/ Thai Palm Oil Industry*. MSc. Thesis, Wageningen University.